8-2004

Compressed Air-Driven Tests of a Prototype TurbX^{TM} Engine

Frederick John Mottley
University of Tennessee - Knoxville

To the Graduate Council:

I am submitting herewith a thesis written by Frederick John Mottley entitled "Compressed Air-Driven Tests of a Prototype TurbX^{TM} Engine." I have examined the final electronic copy of this thesis for form and content and recommend that it be accepted in partial fulfillment of the requirements for the degree of Master of Science, with a major in Mechanical Engineering.

Rao V. Arimilli, Major Professor

We have read this thesis and recommend its acceptance:

Jeffrey W. Hodgson, David K. Irick

Accepted for the Council:
Carolyn R. Hodges

Vice Provost and Dean of the Graduate School

(Original signatures are on file with official student records.)

To the Graduate Council:

I am submitting herewith a thesis written by Frederick John Mottley entitled "Compressed Air-Driven Tests of a Prototype TurbX™ Engine". I have examined the final electronic copy of this thesis for form and content and recommend that it be accepted in partial fulfillment of the requirements for the degree of Master of Science, with a major in Mechanical Engineering.

Rao V. Arimilli
Major Professor

We have read this thesis and
recommend its acceptance:

Jeffrey W. Hodgson

David K. Irick

Acceptance for the Council:

Anne Mayhew
Vice Chancellor and Dean of
Graduate Studies

(Original signatures are on file with official student records.)

Compressed Air-Driven Tests of a Prototype TurbX™ Engine

A Thesis

Presented for the

Masters of Science Degree

The University of Tennessee, Knoxville

Frederick John Mottley

August 2004

This thesis is dedicated to…

My patient wife, Kimberly, who has always been by side encouraging me.

And

My parents, family, and close friends for their guidance, support, love, and enthusiasm.

ACKNOWLEDGEMENTS

I would like to thank my immediate advisor Dr. Rao Arimilli for his guidance throughout my graduate career at the University of Tennessee.

Thanks are also extended to the Oak Ridge National Lab and the National Transportation Research Center for the opportunity to learn from some of the most respected research engineers in the world. Specifically, I would like to thank Jim Conklin and John Andriulli for all the "non-billable" hours you have spent on the project.

I would like to thank the GATE program director at UT, Dr. Jeffrey Hodgson, for the fellowship opportunity focusing my career in automotive technology.

Thanks are extended to the Mechanical, Aerospace, and Engineering Science Department staff, who spent countless hours helping and educating me in a real world experience:

Daniel Graham	Linda Chatham
Steve Hunley	Angela McCarter
Gary Hatmaker	Cheryl Treece

ABSTRACT

A century of research of existing thermodynamic cycles has developed piston engines exceeding 40% efficiency and open cycle gas turbine engines approaching 30% practical efficiency. A breakthrough engine concept has been invented by Dr. Michael Wilson (US Patents 5,966,927 and 6,105,359) and is called the TurbX™ engine. This new engine, operating on the Atkinson cycle, can theoretically increase engine performance and fuel economy, and reduce emissions as compared to the open cycle gas turbine.

The TurbX™ engine implements a constant volume, continuous combustion process in rotating turbo-machinery. Based on a theoretically ideal thermodynamic analysis, this novel innovation will always have a higher thermal efficiency than a typical gas turbine at the same compression ratio. This particular concept has the inherent capability of easily varying the load with very simple controls.

The purpose of this study was to determine experimentally the non-fueled or "air driven" performance characteristics of the prototype TurbX™ engine. The results of this study will be presented and discussed.

Results of loaded tests indicate that with lower gap settings the engine has negative torque-speed characteristics similar to those of gas turbine engines. Although air driven tests were limited to combustion chamber pressures of up to 345 kPa, the prototype engine did not produce the anticipated torque values as envisioned by the inventor. Poor torque output was indicative of the excess leakage prevalent across the rotor/stator gap.

It is recommended that TurbX™ design changes should address a better way to control the gap setting between the rotor and two stators, as well address blade angle and expansion passage designs to reduce the losses associated with poor air-incidence angles.

TABLE OF CONTENTS

Chapter		Page
I	INTRODUCTION	1
II	PROBLEM STATEMEMENT	4
III	THEORY	6
IV	EXPERIMENTAL TEST FACILITY	13
	Physical description of TurbX™	13
	Gap Adjustment	17
	Operation	18
	Couplings	19
	Torque Transducer	20
	Volumetric Digital Gas Flowmeter	21
	Data Acquisition	22
	Test Frame	23
	Engine Dynamometer	25
V	TEST PROCEDURE	28
	Free-Spinning Compressed Air Driven Tests	28
	Loaded Compressed Air Driven Tests	29
VI	RESULTS AND DISCUSSION	30
	Free-Spinning Test Results	30
	Loaded Test Results	35
VII	CONCLUSIONS	38
	LIST OF REFERENCES	40
	APPENDICIES	43
	APPENDIX A	44
	APPENDIX B	45
	APPENDIX C	46
	APPENDIX D	48
	APPENDIX E	50
	APPENDIX F	52
	VITA	53

LIST OF TABLES

Table		Page
4.1	Coefficient of Thermal Expansion for Common Metals……..	16

LIST OF FIGURES

Figure		Page
3.1	Temperature-entropy and pressure-volume diagrams for the Atkinson (1-2-3-4-1), Brayton (1-2-3`-4`-1), and Otto (1-2-3-4``-1) cycles, all with equal heat addition and compression ratio..……...	7
3.2	Ideal Atkinson cycle always has a higher ideal efficiency than the Brayton cycle……	9
3.3	The Holzwarth Cycle……..	11
3.4	The Holzwarth Explosion Engine……...	11
4.1	Flow Diagram and Instrumentation for Unfired Testing of the TurbX™ Engine……..	14
4.2	Top View of the TurbX™ Engine……..	15
4.3	Bottom View of the TurbX™ Engine……	17
4.4	Thomas® Miniature Coupling……	19
4.5	Magtrol Torque Meter……	20
4.6	Laminar Flow Element and Read Out Device……	21
4.7	Backplane and 5B Modules Used in Data Acquisition……..	22
4.8	PCI Card Used in Data Acquisition……	23
4.9	The LabVIEW Virtual Instrument Used in TurbX™ Testing……	24
4.10	Three-Dimensional CAD Model of the Test Frame……...	26
4.11	The TurbX™ Test Rig……	27
6.1	Free-Spinning Speed Characteristics of the Air-Driven TurbX™ Engine and the Testing System…….….	31
6.2	Free-Spinning Temperature Drop Characteristics of the Air-Driven TurbX™ Engine and the Testing System……..32	

6.3 Free-Spinning Volumetric Air Flowrate Characteristics of the Air-Driven TurbX™ Engine and the Testing System……..… 34
6.4 Free-Spinning Torque Characteristics of the Air-Driven TurbX™ Engine and the Testing System……... 35
6.5 Loaded Torque Speed Plot for TurbX™ Prototype…… 36
B.1 Thomas Miniature Couplings Data Sheet……... 45
D.1 Laminar Flow Meter Calibration Certificate…….. 48
D.2 Laminar Flow Meter Calibration Information…… 49
F.1 Barbour Stockwell Air Turbine Dynamometer Performance……. 52

LIST OF SYMBOLS

BSAT	Barbour Stockwell air turbine
^{o}C	degree Celsius
cfm	cubic feet per minute [ft^3/min]
c_p	specific heat, constant pressure [kJ/(kg·K)]
c_v	specific heat, constant volume [kJ/(kg·K)]
DC	direct current
^{o}F	degree Fahrenheit
P_a	absolute pressure
P_{gc}	pressure of the gasses inside the combustion chamber
k	specific heat ratio, c_p/c_v
K	kelvin [K]
kPa	kilopascal
ksi	kilo pounds per square inch, 1000 x [lb/in^2]
kS/s	kilosamples/second
kW	kilowatt
LFM	laminar flow meter
η	efficiency
NI	National Instruments
NTRC	National Transportation Research Center
ORNL	Oak Ridge National Laboratory
psi	pounds per square inch [lb/in^2]
psig	pounds per square inch, gauge [lb/in^2]
r_c	compression ratio
rpm	revolutions per minute
s	entropy [kJ/kg·K]
slpm	Standard liters per minute

T	temperature [K]
T_{gc}	Temperature of the gasses inside the combustion chamber [K]
T_{ge}	Temperature of the gasses at the last stator expansion chamber [K]
UTK	University of Tennessee, Knoxville
VDC	Direct current volts
VI	Virtual Instrument
W	watt

CHAPTER I

INTRODUCTION

A century of research of existing thermodynamic cycles has developed piston engines exceeding 40% thermal efficiency and open cycle gas turbine engines approaching 30% overall efficiency. Even the slightest increase in efficiency can have dramatic economic and environmental impacts. For this reason, significant emphasis has been placed recently on modifying engine designs to squeeze out even the slightest increase in thermal efficiency.

Dr. Michael A. Wilson has invented a new concept internal combustion engine called the TurbX™. Using his own resources, he designed and fabricated a prototype TurbX™ engine. Two patents were awarded in 1999 [1] and 2000 [2], totaling 41 claims. The engine is comprised of a single rotor, boxed in by two stators. The rotor bearing supports are located in the stators. As the working fluid moves with the rotor, an entire thermodynamic cycle is executed. Intake, compression, ignition, expansion and scavenging processes are completed for each revolution of the rotor. In this sense, this engine is different from gas turbine engines in which the individual processes occur in different physical components. Unlike reciprocating engines, this engine operates with continuous combustion, similar to a rotary gas turbine. The tested prototype TurbX™ engine was designed by the inventor to produce 15kW of power at a design speed of 20,000 rpm.

This engine is claimed to have higher efficiency and fuel economy relative to production engines of similar size. Further, TurbX™ has an advantage over reciprocating engines in that it has fewer moving parts, resulting in lower manufacturing, machining and long-term maintenance costs. This engine has the potential to compete with power generating devices in stationary power and transportation applications. TurbX™ could supply onsite gen-set capabilities in military applications [3], or even as onsite power supplies for individual homes.

In this engine the heat addition process may be approximated as a constant volume process. Ideally, the TurbX™ cycle is best described by the Atkinson thermodynamic cycle. For a given compression ratio, this cycle would have higher thermal efficiency than both the Otto (typical US automobile engine) and Brayton (gas turbine) cycles. Reciprocating Otto cycle piston engines have been designed to operate on the Atkinson cycle, but are often associated with increased costs and geometric complexities such as delayed intake valve operation and offset crankshafts. Power density suffers because only a portion of the total displacement volume is filled with a fresh charge of air [4]. The efficiency limitations of modern gas turbine engines are directly related to high turbine operating temperatures. In gas turbines, the first row of rotor blades in the expansion turbine are constantly exposed to high-temperature high-pressure conditions. Mechanisms of failure seen in gas turbine alloys are directly related to these conditions include fatigue, creep, hot corrosion, and high-temperature oxidation. In contrast, the mechanical piece (rotor) of the TurbX™ engine is only intermittently exposed to the high-pressure high-temperature conditions of its rotating combustion chamber with combustion limited to a portion of each rotation of the rotor. Thus, the mean temperature of the rotor is far less than the steady temperature encountered by the turbine stage of modern gas turbine engines. This allows higher temperatures to be utilized in the TurbX™ combustion chamber, resulting in higher efficiency.

Dr. Wilson started on the TurbX™ concept in 1983 and had further developed the concept in 1995. In 1997 the proof of concept was completed, with a prototype available in 1998. Following the two patents, he approached several companies and venture capitalists to move the technology forward. In the process, it was clear that demonstrated positive performance test results of the prototype engine, preferably by a third party, were necessary to continue further development activity.

Oak Ridge National Laboratory (ORNL) and the University of Tennessee (UTK) were particularly interested in the concept. With some funding from the Tennessee State Energy Partnership Program, a joint effort between the two parties was established to determine performance characteristics of the prototype engine and to make recommendations. Testing was performed in Knoxville, TN at the National Transportation Research Center (NTRC), a joint effort involving ORNL and UTK.

CHAPTER II

PROBLEM STATEMENT

The TurbX™ engine had never been tested independently, therefore engine parameters had to be determined. Choosing appropriate instrumentation within time and budget constraints was important. Knowing the power output and fuel type, the theoretical mass flow rates of fuel and air could be determined, to aid in sizing the instrumentation. Data was collected with LabVIEW, a data acquisition software program by National Instruments. Parameters of interest included: output shaft torque and speed, volumetric flow rates of inlet air and fuel, temperatures inside the engine such as the combustion chamber, the last stage of the expansion chamber, and the gap setting between the rotor and two stators. Software for the data acquisition system had to be written before any tests were conducted.

A test stand had to be designed and fabricated to support this prototype engine and instrumentation while being tested up to speeds of 20,000 rpm. It needed to be sturdy, yet also easily accessible. Safety compliance also had to be met while at the NTRC facility. Several independent reviews by NTRC staff during the design and fabrication process were conducted.

In the proposed test plan, two distinct tests were recognized, an un-fueled and fueled test. The unfueled test is referred to as the *air driven* test, and the fueled test is referred to as the *fired* test. Initially, the air-driven test was performed using compressed air to drive the engine. Compressed air was fed into the spark plug port and was allowed to expand in the engine through the stator-rotor passages, producing work. The air driven tests were conducted to determine the following: minimum combustion chamber pressure required to develop torque for a given speed, validity of the assumed theory, specific recommendations to the inventor, and overall familiarity with the engine prior to fueled tests.

The fired test used technical grade gaseous methane (CH_4) as the fuel. The purpose of the methane fueled fired test was to measure engine performance characteristics as a function of speed. Characteristics of interest included output torque, fuel flow rate, and other thermodynamic parameters including combustion chamber gauge pressure and temperature. The detailed results of the fired test are presented in a thesis by Kurt Erickson for a Masters of Science Degree at the University of Tennessee [5].

CHAPTER III

THEORY

The TurbX™ engine can be considered to operate on the ideal air standard Atkinson cycle. The cycle is shown on T-s and p-υ coordinates in Figure 3.1. The engine implements a constant volume continuous combustion process.

The Atkinson cycle, *1-2-3-4-1,* starts with adiabatic compression of the working fluid in the process from *1-2*, followed by heating at constant volume to the high pressure and temperature at state *3*. The fluid undergoes adiabatic expansion process, *3 - 4*, and then cools at constant pressure from *4-1* to complete the cycle.

From Figure 3.1, it can bee seen that for the same compression ratio and the same heat addition, the Atkinson cycle will always have a higher thermal efficiency than a typical gas turbine (Brayton) cycle because the constant volume heat addition results in a higher expander inlet temperature and pressure than the constant pressure heat addition process of the corresponding Brayton cycle (*1-2-3`-4`-1*).

Also, the Atkinson cycle efficiency is higher than that of the Otto cycle because expansion occurs all the way down to ambient pressure (4”-4’). Thus no potential energy is wasted during the exhaust process from a pressure higher than ambient as occurs in the Otto cycle (4”-4).

In the following it will be shown that that the thermal efficiency of the ideal air-standard Atkinson cycle is always higher than the thermal efficiency of the ideal Otto, Diesel, or Brayton cycles for a given compression ratio.

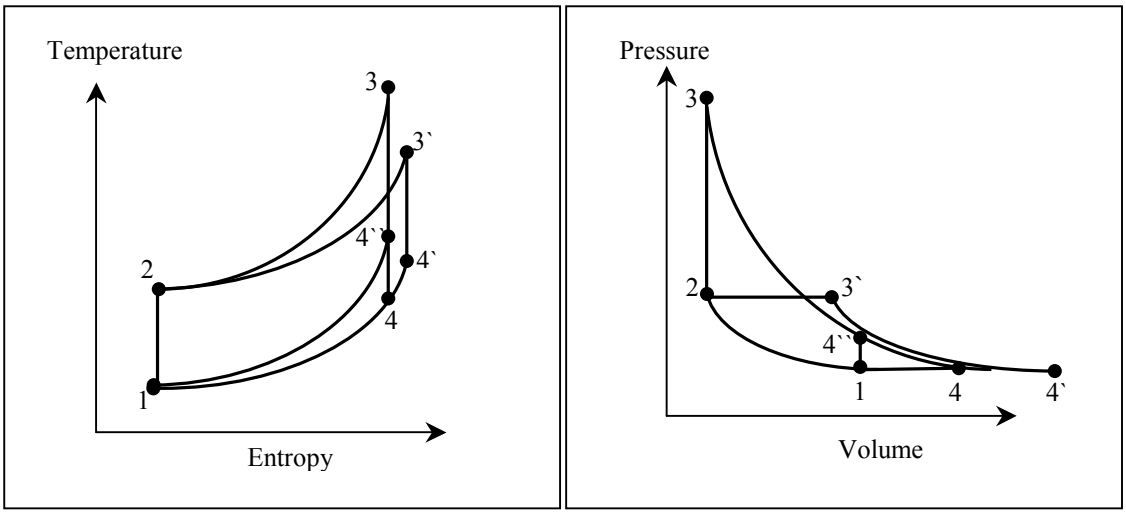

Figure 3.1 Temperature-entropy and pressure-volume diagrams for the Atkinson (1-2-3-4-1), Brayton (1-2-3`-4`-1), and Otto (1-2-3-4``-1) cycles, all with equal heat addition and compression ratio.

The standard definition of thermal efficiency is:

$$\eta = 1 - \frac{\text{heatrejected}}{\text{heatsupplied}} \tag{1}$$

From the T-s or p-υ diagram, the thermal efficiency of the ideal Atkinson cycle is [6]:

$$\eta_{Atk} = 1 - \frac{C_p(T_4 - T_1)}{C_v(T_3 - T_2)} = 1 - \frac{k\left[{}^{T_4}\!/_{T_1} - 1\right]}{{}^{T_2}\!/_{T_1}\left[{}^{T_3}\!/_{T_2} - 1\right]} \tag{2}$$

By definition:

$$\frac{T_4}{T_1} = \frac{v_4}{v_1} = \frac{v_3}{v_1}\frac{v_4}{v_3} = \frac{v_2}{v_1}\frac{v_4}{v_3} = \left(\frac{T_2}{T_1}\right)^{\frac{1}{1-k}}\left(\frac{T_4}{T_3}\right)^{\frac{1}{1-k}} = \left(\frac{T_4}{T_1}\right)^{\frac{1}{1-k}}\left(\frac{T_2}{T_3}\right)^{\frac{1}{1-k}} = \left(\frac{T_3}{T_2}\right)^{\frac{1}{k}} \tag{3}$$

Substituting equation 3 into equation 2 results in the following:

$$\eta_{Atk} = 1 - \frac{k\left[\left({}^{T_3}\!/_{T_2}\right)^{1/k} - 1\right]}{{}^{T_2}\!/_{T_1}\left[{}^{T_3}\!/_{T_2} - 1\right]} \tag{4}$$

For isentropic compression, the temperature ratio T_2/T_1 is a function of the compression ratio r_c as follows:

$$\frac{T_2}{T_1} = \left(\frac{v_2}{v_1}\right)^{1-k} = r_c^{1-k} \tag{5}$$

$$where \quad r_c = \frac{v_1}{v_2}$$

As it is desirable to use the parameter of the ratio of turbine inlet temperature T_3 to the compressor inlet temperature T_1, which will be abbreviated as T^*, equation 4 can be written as:

$$\eta_{Atk} = 1 - \frac{k\left[(T^*)^{\frac{1}{k}}(r_c)^{\frac{1-k}{k}} - 1\right]}{\left[T^* - (r_c)^{k-1}\right]} \tag{6}$$

Note that the thermal efficiency of an Atkinson cycle is a function of load or heat added, T^*, as well as the compression ratio.

The ideal simple Brayton cycle thermal efficiency can be derived from the general definition of equation 1 as [6]:

$$\eta_{Bray} = 1 - \frac{T_1}{T_2} = 1 - (r_c)^{1-k} \tag{7}$$

Note that the ideal simple Brayton cycle thermal efficiency is a function of the pressure ratio only, and is independent of the load, or the turbine inlet temperature. Equation 7 also represents the ideal cycle efficiency of a piston engine operating on the ideal Otto cycle [4]. In Figure 3.2 the ideal Atkinson cycle thermal efficiency is plotted as a function of compression ratio and for three values of the maximum to minimum temperature ratio (load) T^*=3, 4, 5 and 6.

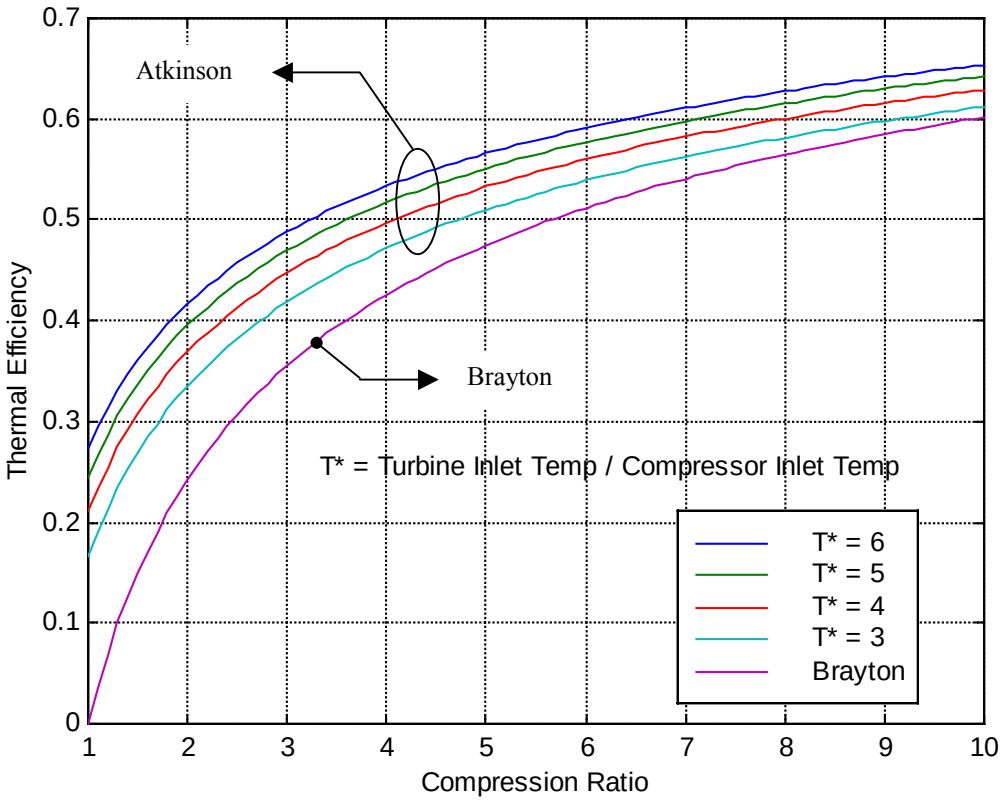

Figure 3.2. Ideal Atkinson cycle always has a higher ideal efficiency than the Brayton cycle.

It can be seen that the ideal Atkinson cycle has a higher thermal efficiency than the ideal Brayton or Otto cycle when compression ratios are equal.

A recent study of constant-volume combustion gas turbine efficiency was reported by Venturini and Varella [7]. They analyzed and compared modern Brayton cycles engines to gas turbines operating under the constant volume combustion cycle, developed by Dr. Holzwarth of Germany in the early 20th century. This is of particular interest to the TurbX™ engine because the Holzwarth cycle is equivalent to the Atkinson cycle, both having heat addition during a constant-volume process.

Dr. Hans Holzwarth, whose initial experiments started in 1905, developed a gas 'explosion' turbine engine. In this system (Figure 3.3), a compressor introduced a charge of air and fuel into a constant-volume combustion chamber. After ignition, the hot, high-pressure gas escaped through spring-loaded valves into nozzles directed against the blading of a turbine. The valves remained open until the gas was discharged, at which point a fresh charge was introduced into the combustion chamber. Since the pressure increase in the compressor was only about one-fourth of the maximum pressure reached after combustion, the unit could operate, delivering net work even though the compressor efficiency was low. From the first prototype built between 1906 and 1908, Holzwarth and various collaborators continued to develop the explosion turbine for more than 30 years until it was eventually superseded by the modern constant-pressure gas-turbine engine.

The thermal efficiency for the Holzwarth cycle has been shown to be significantly higher than the gas turbine operating under the Brayton cycle, particularly at low compressor pressure ratios. Consequently, the Holzwarth concept has potential advantages over the Brayton cycle, especially if gas turbines use smaller compressors to gain efficiency. Figure 3.4 depicts a picture of the Holzwarth Engine.

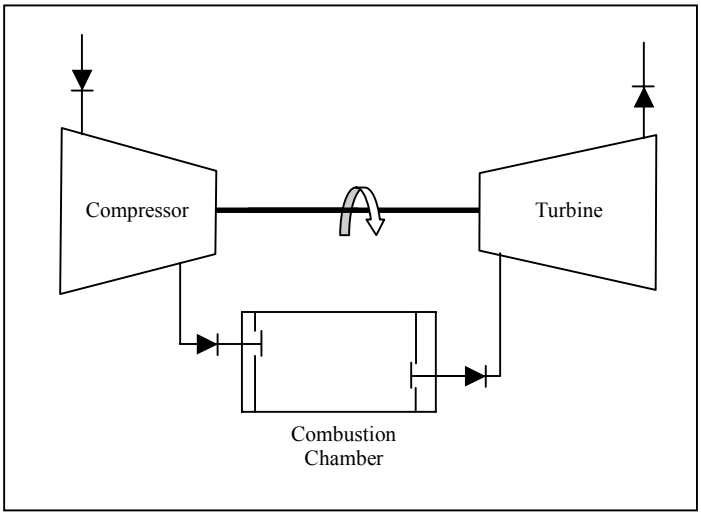

Figure 3.3. The Holzwarth Cycle

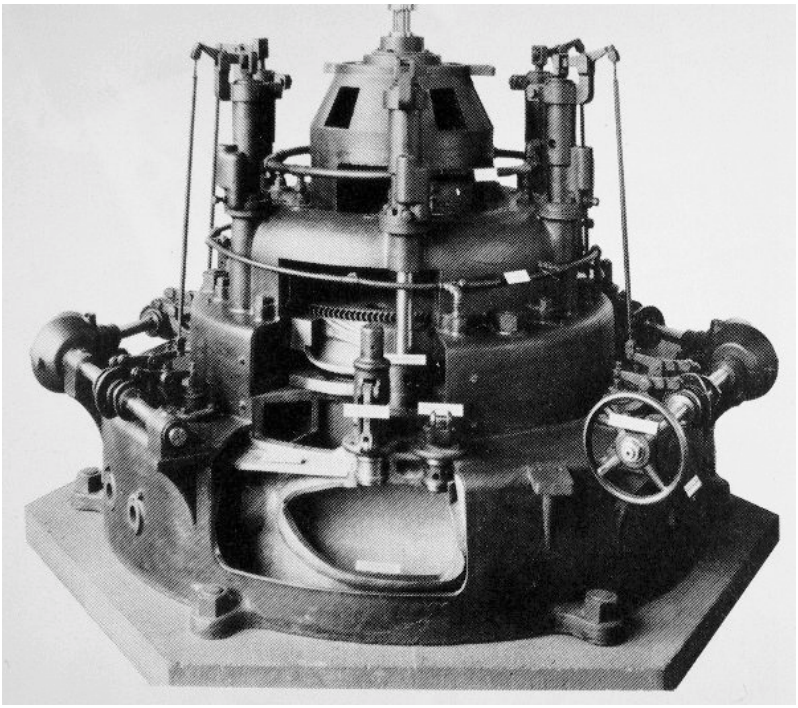

Figure 3.4. The Holzwarth Explosion Engine

Another recent study by Hutchins and Metghalchi [8] presents the energy and exergy analysis of the pulse detonation engine. The pulse detonation engine uses a detonation wave instead of a deflagration wave for the combustion process. This high-speed supersonic combustion wave reduces overall combustion duration resulting in a nearly constant volume energy release process. This constant volume process is again similar to the theoretical TurbX™ engine combustion cycle. Comparisons shown by Hutchins and Metghalchi indicate that for the same pressure ratio the pulse detonation engine has better efficiency and exergic efficiency than the gas turbine system.

CHAPTER IV

EXPERIMENTAL TEST FACILITY

In order to effectively measure the performance characteristics of the prototype TurbX™ engine, expected to operate at speeds up to 20,000 rpm, a special test system had to be built. Since the maximum operating speed of 20,000 rpm is considerably higher than the speed of typical reciprocating internal combustion engines, several precautionary measures had to be taken into account during the design and fabrication of the test facility to ensure the safety of all personnel involved. This system was designed in a *vertical* shaft orientation, and consisted of the dynamometer, torque meter, and TurbX™ engine. A flow diagram of the instrumentation is shown on Figure 4.1. The limited financial resources available were expended on items of most significance to the overall project, namely, the torque and laminar flow meters to determine the net power output of the engine accurately.

Physical Description of the TurbX™ Engine

The prototype TurbX™ engine was designed by the inventor to produce 15 kW of power at 20,000 rpm. For brevity, this engine will be referred to simply as TurbX™ in the rest of this thesis. The design was based on the assumptions that (1) complete combustion occurs, (2) expansion processes are isentropic, (3) leakage losses between the rotor and the stators are negligible, (4) heat losses are negligible, and (5) flow is aligned correctly with the fixed angles of the rotor blades at the exit of every expansion stage.

TurbX™ is compact and lightweight relative to other production engines producing the same amount of power, having dimensions of 19.05 cm (7.5 inches) square and a thickness of 3.8 cm (1.5 inches), with a mass of only 9 kg (20 lb_m). The engine's structure consists of four primary components: a rotor, two stators, a drive shaft, and a housing unit. A picture of the engine is seen in Figure 4.2. The key engine components are all

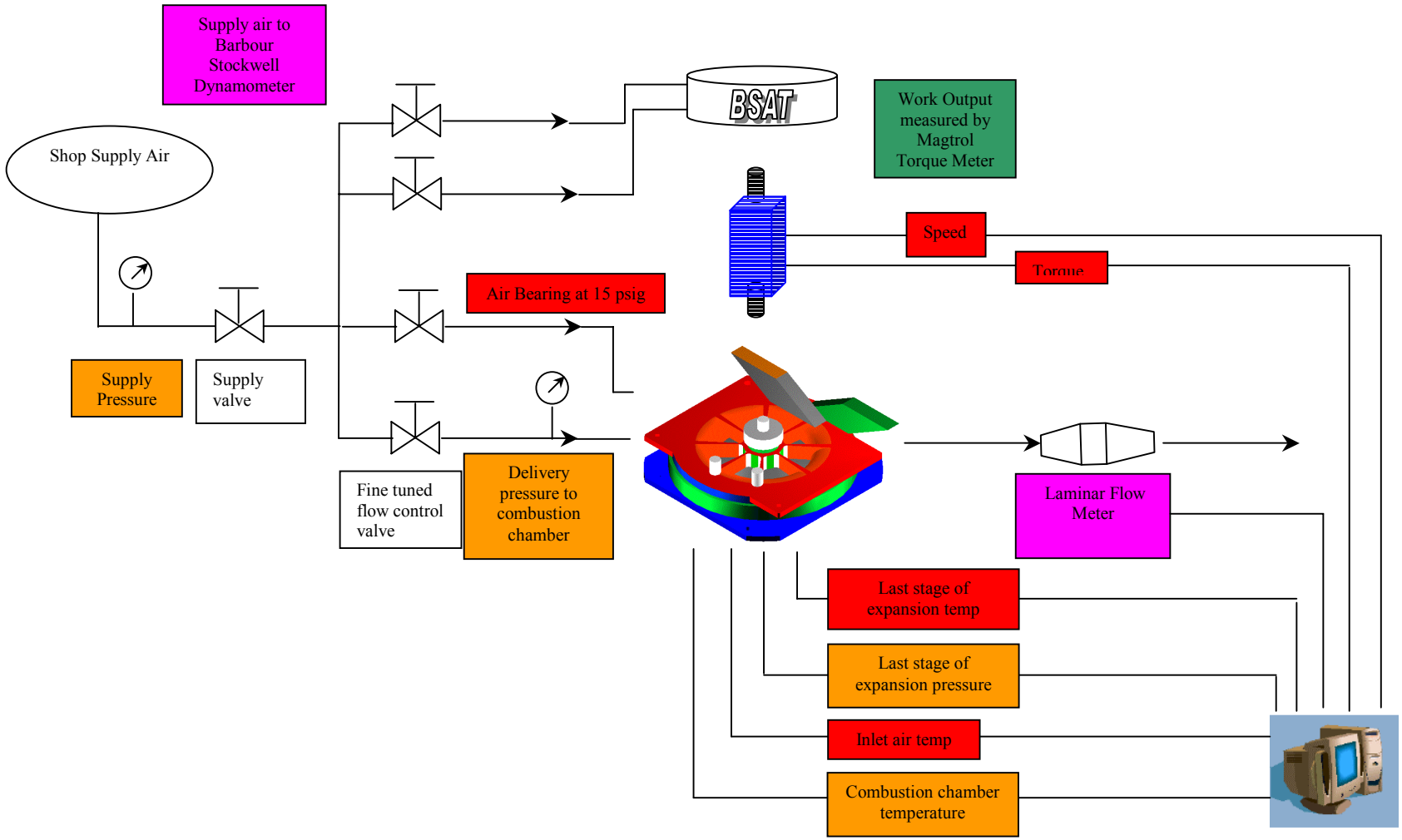

Figure 4.1. Flow Diagram and Instrumentation for Unfired Testing of the TurbX™ Engine

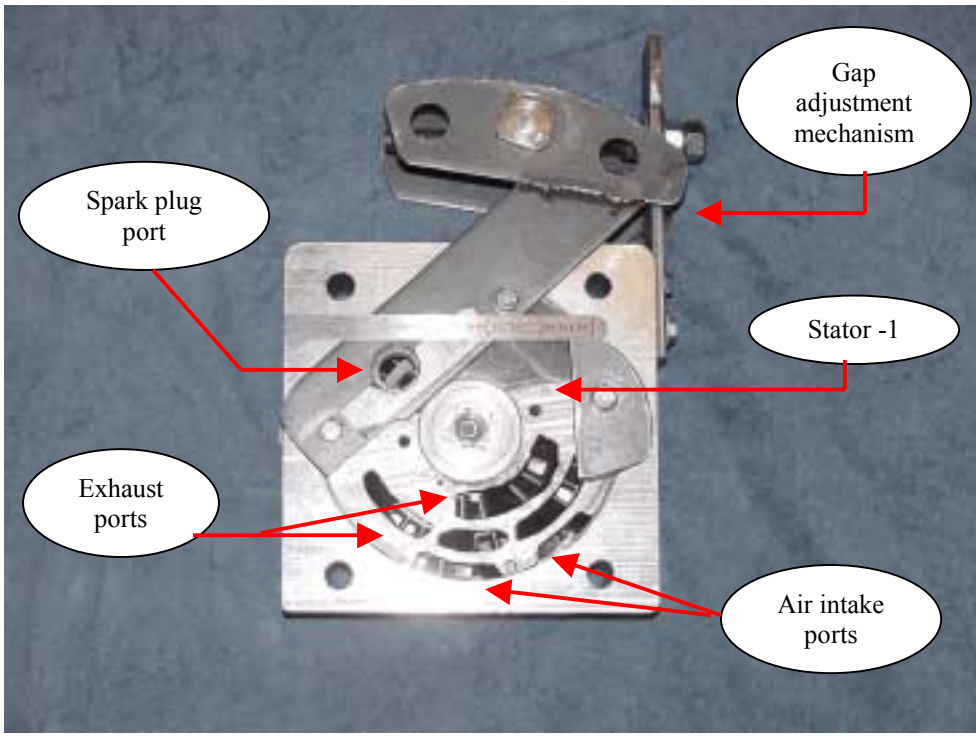

Figure 4.2. Top View of the TurbX™ Engine

fabricated out of a metal alloy, Invar-36, because of its low coefficient of thermal expansion. Invar properties are shown in Table 4.1, relative to some common metals. Invar is often used in conjunction with high expansion alloys, in applications where a motion is desired with temperature changes, such as bimetallic thermostats. This alloy is used to minimize galling of the rotor and stators of the engine, as the prototype has no cooling system in its present design. Furthermore, the two faces of the rotor and opposing faces of the two stators are machined to minimize the possibility of stator-to-rotor contact.

The rotor and the output shaft, located between the two stators, are the only rotating components in this engine; all other components are stationary. The rotor is

Table 4.1. Coefficient of Thermal Expansion for Common Metals

Metal	**Coefficient of Thermal Expansion x 10^{-6} at 20 ^{o}C (K^{-1})**
Invar-36	1.7
Aluminum	24
Iron	12
Carbon steel	13

supported by the two stators with an air bearing that is supplied with pressurized air to create a thin air-bearing film. For the purpose of this thesis it is assumed this air bearing allows nearly frictionless rotation of the rotor at all speeds. Although this is probably not true, as pressurized air does have friction, determining the friction of the air bearing is beyond the scope of this project. A detailed description of the operation of the engine, as envisioned by the inventor, can be found in Erickson [5].

Natural gas was selected as the fuel source for this engine. The fuel injector ports are threaded 0.3175 cm (0.125 inch) diameter holes, just prior to the combustion chamber, as depicted in Figure 4.3. The ignition source is a common spark plug threaded into a port in the combustion chamber. Note that the spark plug, intake, and exhaust all lie on the same side of the engine, on stator-1.

The square shaped housing holds the main components and gap adjusting mechanism. It is bored-out to roughly the size of the stators (12.7 cm), and then internally threaded.

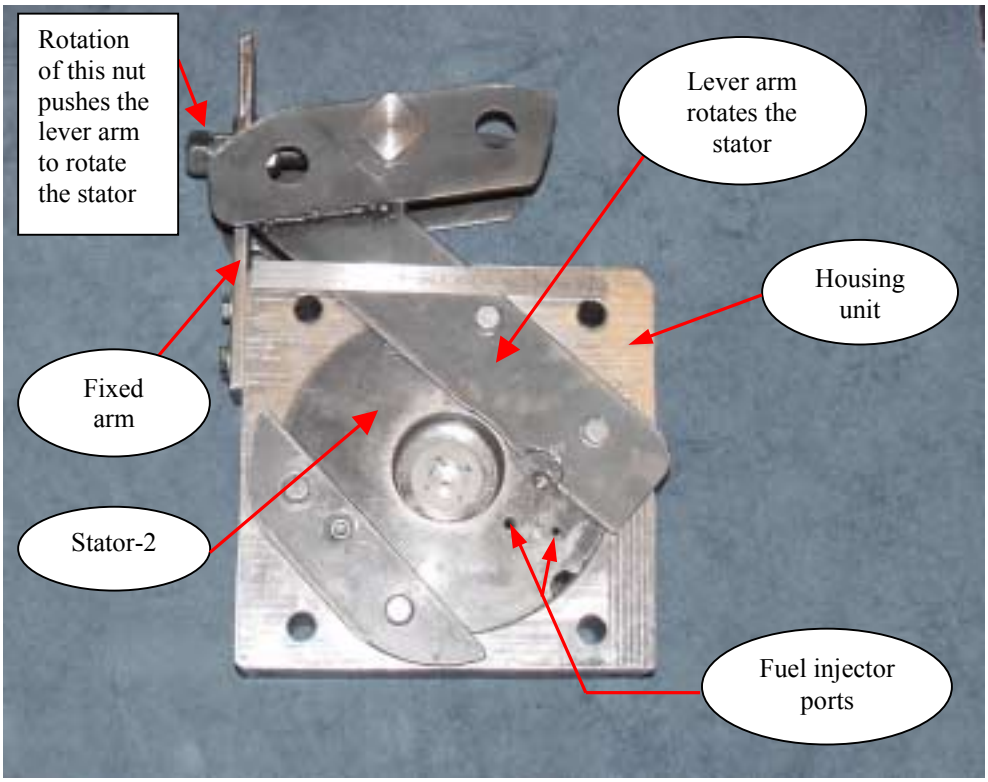

Figure 4.3. Bottom View of the TurbX™ Engine.

The stators then screw into the housing unit from both directions (top and bottom) in such a fashion that when both of them are rotated in the same direction simultaneously, they move closer to the rotor. The determination of the actual *gap*, the spacing between the stators and the rotor, is described next.

Gap Adjustment

Adjustment of the air gap between the rotor and stators is accomplished via two conjoined lever arms, each one connected to its respective stator. By turning the nut on the fixed arm, the length of the adjusting bolt can be varied. This turns the two stators toward each other, relative to the housing unit, thereby reducing the gap between the rotor and stators. Thus the gap may be varied by simply tightening or loosening the nut.

To initialize the air gap with the engine, the gap was set at a relatively large value and then compressed air is supplied to the air bearing. By freely rotating the output shaft by hand while simultaneously turning the nut on the fixed arm, the two stators were rotated until the output shaft encountered a slight resistance. The resulting gap is designated as G_0, indicating near contact with the rotor. At this point, the nut was rotated eight full revolutions (G_8) in the opposite direction to pull the stators apart. The nut is then rotated again in the initial direction by five full revolutions (G_3), bringing the stators closer. For each revolution of the nut, the gap on each side of the rotor is 0.000004 m (0.0002”). Backlash in the control mechanism made it difficult to determine the exact gap width. From G_3 the nut is advanced one full revolution to move the stators closer, making the gap smaller and the resulting gap is designated as G_2. One additional revolution results in the final gap, G_1. Tests were then conducted at these gap values of G_3, G_2, and G_1 (smallest).

Operation

All phases of the Atkinson power cycle, suction, combustion, and expansion are completed by the three main components of TurbX™, the two stators and rotor. The fan blades located on the outermost periphery of the TurbX™ rotor sweep the air from the two intake ports into the engine. This air is then mixed with fuel delivered by the injector port located on stator-2, and induced into the combustion chamber by the rotor and ignited by the spark plug. The rotor then carries the burning air-fuel mixture to the first (of seven) stator expansion passage. The burning air-fuel mixture entrapped in the space between adjacent blades of the rotor continues to burn without expansion as it moves from the combustion chamber to the first stator expansion passage. This heat addition process occurs at constant volume, although the volume is rotating.

As the high-temperature, high-pressure gas passes through the first stator expansion passage, the available energy is partially converted into kinetic energy. The gas jet accelerates through the first stator expansion passage making a 180^o turn and

reenters the rotor, hitting the concave turbine blades. The blades convert this energy into work. The gas again reenters another stator passage, but this time on the other side of the rotor, into stator-1, and again swirls 180^{o} for yet another pass through. A total of 7 expansion passages are machined out of each stator, where the gas expands in a helical path. Upon the last expansion passage, the gas then exits the exhaust port, located on stator -1. A depiction and detailed process of the fluid flow is presented by Erickson [5].

Couplings

The couplings used in this experiment were purchased to withstand radial stresses associated with a rotational speed of 20,000 rpm, and yet not be an overbearing mass on the total inertia of the system. Thomas® Miniature couplings, a division of Rexnord, were chosen to mate the two sets of shafts. Thomas offers clamping hubs that are an integral part of the coupling, and assure positive fit on the shafts. Dynamically balanced couplings were needed, so two Thomas model CBC-62 couplings were chosen. A picture of a coupling is shown in Figure 4.4, with further details shown in Appendix B.

Figure 4.4. Thomas® Miniature Coupling

Torque Transducer

The torque measuring device for testing the TurbX™ engine was purchased from Magtrol, of Fribourg, Switzerland and has several unique characteristics suitable for testing TurbX™. Foremost, this instrument has a speed rating of 50,000 rpm, and has shaft speed and torque outputs. The speed output is an open collector pulse generator, with input voltages of up to 30 VDC. Torque output is 0 to ±10 VDC, which is centered on 0 and corresponds linearly to ± 10 N-m. The linearity and hysteresis error is less than 0.1% of full scale. The transducer consists of a stainless steel shaft having smooth ends and an aluminum housing containing the guide bearings as well as the electronic measuring conditioner. The stainless steel shaft has a mass of 1.2 kg with a mass moment of inertia of 31.8×10^{-6} kg·m^2 and makes for a sensitive torque measuring system. Of all the instrumentation, this piece needed to be the one most precise. Without precision in the torque meter, a quantifiable torque (thus power) could not be ascertained accurately, thus a majority of capital resources were used to acquire this device. A picture of the Magtrol model TM-207 torque meter is seen in Figure 4.5.

Figure 4.5. Magtrol Torque Meter

Volumetric Digital Gas Flowmeter

In order to measure the air flowrate through the TurbX™, a laminar gas flow meter calibrated for air was used. CME, a division of Aerospace Control Products of Davenport, Iowa manufactured this instrument, and calibrated it to air at 0-1,200 SLPM, with 0.17% error at full scale. In order to determine this span of 1,200 SLPM, a calculation for determining the airflow rate requirements is shown in Appendix C. The 40L series provides digital readout as well as a 0-2 VDC analog output for data acquisition on the computer. A port for a Swagelok® compression fitting was also available for an accurate temperature measurement at the center of the instrument housing. It should be pointed out that, during cold flow tests, this flow meter was actually installed downstream of the engine, measuring airflow rate through the exhaust stream. A picture of the laminar flow element is in Figure 4.6. Additional information is provided in Appendix D.

Figure 4.6. Laminar Flow Element and Read Out Device

Data Acquisition

The acquisition of test data at the NTRC test cell was handled by the National Instrument (NI) 5B series analog signal conditioning modules [9]. These modules were installed into an 8-channel backplane that connected to the data acquisition device (Figure 4.7), providing assorted isolated signal conditioning on a channel-by-channel basis. I/O signals are connected to the backplane of the 5B system, not the individual modules. This feature makes it easy to replace or swap modules. Each individual channel was calibrated using NI's Measurement and Automation Software. The software has the capability to initialize and calibrate each device. The software can also initialize and scale each input channel separately.

After the signals are conditioned by the 5B modules, they are routed to an NI 6052E data acquisition device (Figure 4.8). This device was inserted into an available PCI slot on a Dell Optiplex GX1 desktop computer with a 400 MHz Intel Pentium III® processor. The NI 6052E delivers at a 333kS/s sampling rate, with 8 differential analog inputs, 2 analog output channels, 16-bit resolution, and 8 digital I/O lines.

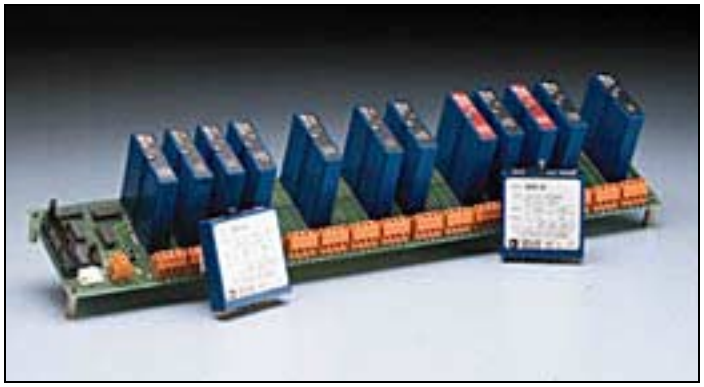

Figure 4.7. Backplane and 5B Modules Used in Data Acquisition

Figure 4.8. PCI Card Used in Data Acquisition

The Dell PC then uses NI's LabVIEW™ Virtual Instruments software to collect digital input and stores it as a delimited text file. LabVIEW™ is a graphical programming language that has been widely adopted for data acquisition and instrument control. The virtual instrument (VI) used in this test cell was designed specifically to test the TurbX engine. A screen shot of the VI interface may be seen in Figure 4.9. It displays and records several testing parameters, including: inlet temperature, inlet pressure, exhaust temperature, exhaust pressure, combustion chamber temperature, combustion chamber temperature, last stage of expansion temperature, engine torque, engine speed. The VI also has the capability to record fuel flow rate for fired testing.

Test Frame

The test frame used to test TurbX™ at the NTRC was fabricated specifically for this engine. Carbon steel, 1-inch stock, slotted C-channel was used as the framing material. This was used primarily because of its low cost, common availability in 8-foot segments, and pre-slotted holes. Off-the-shelf "T" and "L" brackets also simplified connections to equipment and hardware.

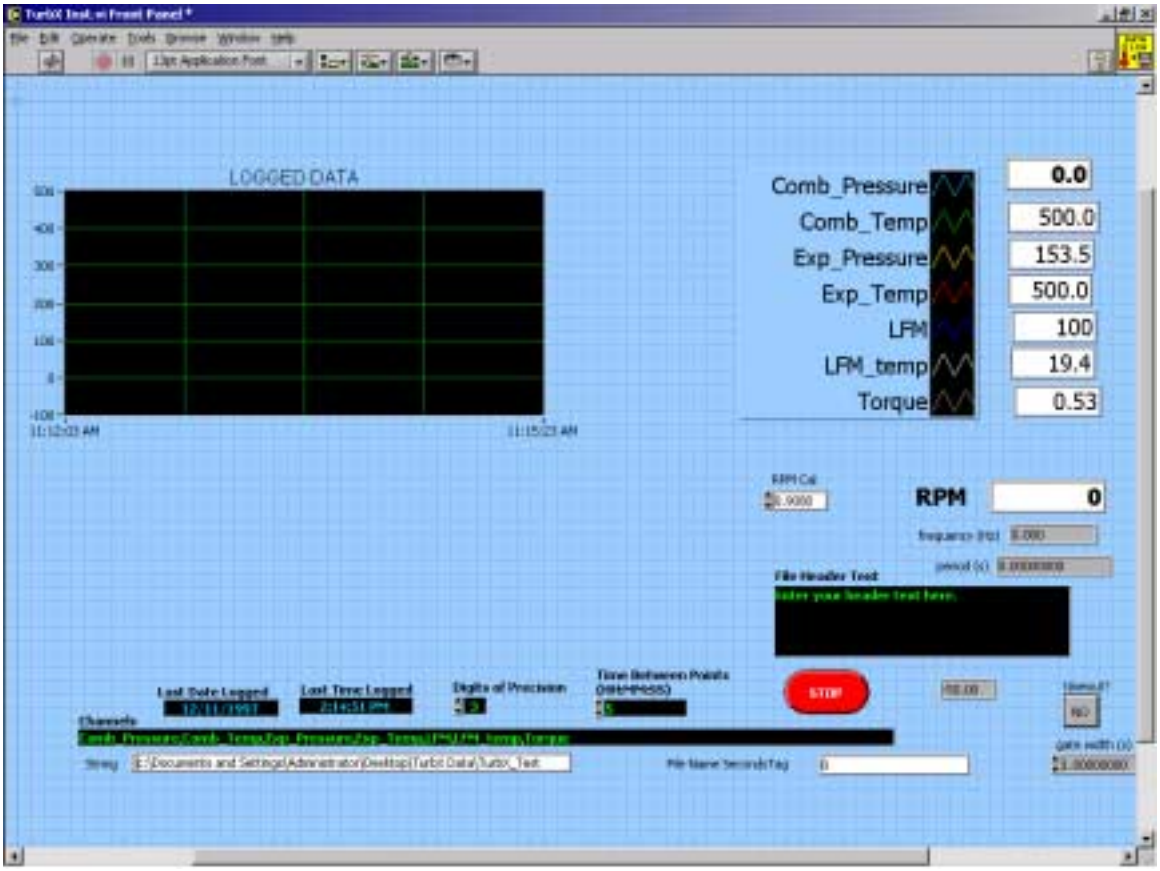

Figure 4.9. The LabVIEW Virtual Instrument Used in TurbX™ Testing

In all, the frame connected to the 1.27 cm thick plate above, then had the torque meter mounted to it, followed by TurbX™ underneath. Several redundant members were also added to the frame to ensure a rigid and stiff system. Even with pre-drilled and slotted holes, much fabrication needed to be done to ensure proper alignment of the rotor, torque meter, and dynamometer shafts, all theoretically spinning at 20,000 rpm. A SolidWorks 3-D mock-up drawing of the frame is shown in Figure 4.10 [10].

Engine Dynamometer

The engine dynamometer incorporated into this test cell was an 8-inch Barbour Stockwell air turbine (BSAT). The BSAT was used to initiate rotation of the TurbX engine during all air-driven tests. This air turbine is manufactured to rotate up to 25,000 rpm, with a total air consumption of 20,388 LPM, at 620 kPa, 23.8 ^{o}C. Therefore, it would be suitable for operating the TurbX engine at the design speed of 20,000 rpm. BSAT is powered by shop supply air to either a clockwise (CW) or counterclockwise (CCW) cupped pelton wheel, directly driving the output shaft of the device. To control the dynamometer, individual gate valves are used to meter inlet pressure to the CW and CCW pelton wheels, respectively. Total cross sectional nozzle area is 2.42 cm^2. The output shaft of the turbine is 1.27 cm in diameter and is connected directly to a Thomas® Coupling. A picture of the BSAT is shown in Figure 4.11. The BSAT turbine was chosen primarily because it was available at no additional cost for use on this project. It had at been used in the centrifuge program at ORNL, and was in storage at the time. Note that this air turbine will only operate in a vertical shaft orientation. Several safety issues associated with using the dynamometer at the NTRC facility have been addressed in Appendix E. Discussions of shaft orientation will be addressed in subsequent chapters. The Barbour Stockwell turbine performance graph is in Appendix F.

The following chapter will be discussing a descrition of how all this equipment was used to effectively measure the output characteristics of the air-driven unfired engine.

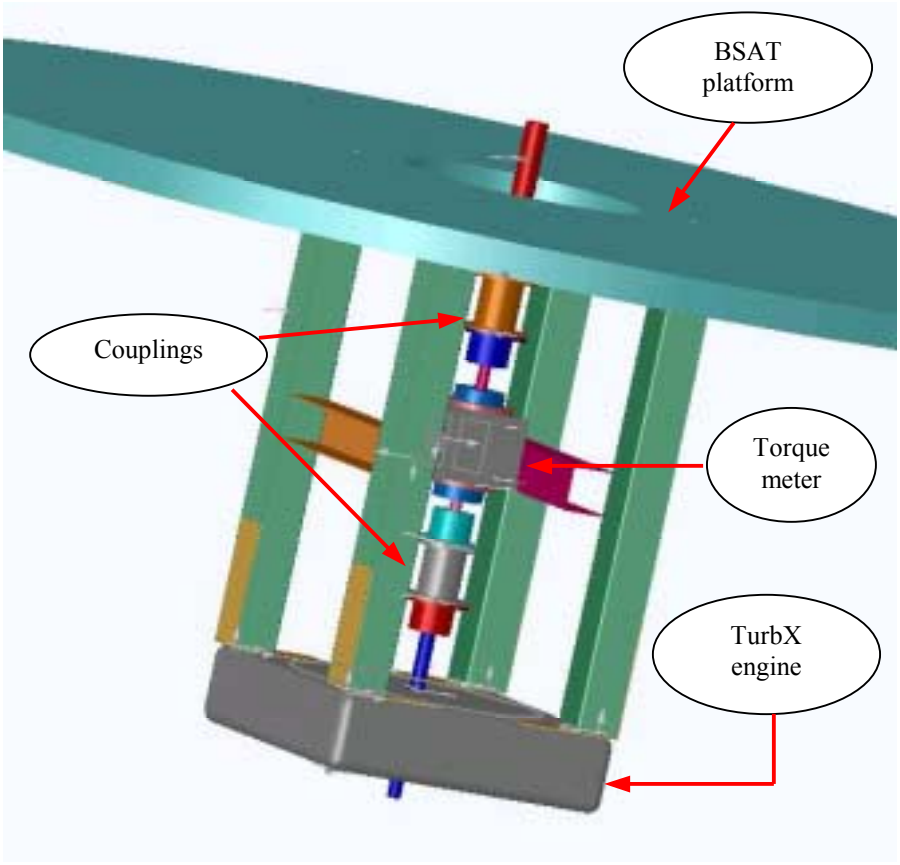

Figure 4.10. Three-Dimensional CAD Model of the Test Frame

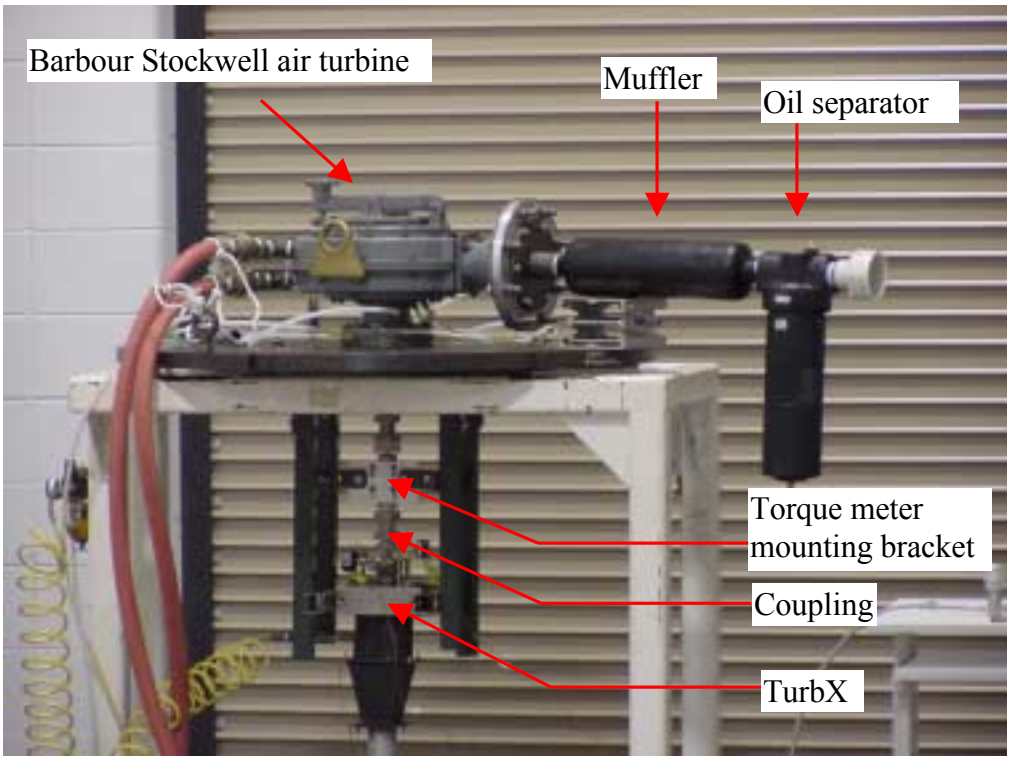

Figure 4.11. The TurbX™ Test Rig

CHAPTER V

TEST PROCEDURE

To initiate the air-driven tests, compressed air was supplied to the TurbX™ at two locations, the spark plug port and the air bearing. Air inlet ports in stator-1 along with the fuel injection ports on stator-2 were completely sealed to prevent room air from entering the engine. The two air inlet ports were sealed with a stiff rubber gasket, and the fuel injectors were plugged with a thread-matching hex bolt to prevent leakage through them. With this arrangement, the air entering the spark plug port is forced to expand through the TurbX™ and exit through the exhaust ports to produce work. The exhaust air flow rate was measured by the laminar flow element. When air is supplied to both the spark plug port and to the air bearing, the laminar flow element measures the sum of these two volumetric air flow rates needed to spin TurbX™ at a constant speed.

The prototype design was such that the rotor is free to slide on the key and bearing shaft. For the engine mounted with a vertical axis of rotation, the rotor is free to slide and rest on the bottom stator (stator-1). Preliminary tests, spinning TurbX™ up to 10,000 rpm, indicated that a minimum bearing air pressure of 276 kPa gauge is required to the air bearing to float the rotor above stator-1.

After the air pressure has been supplied to the lift the TurbX™ air bearing, the oil pump for the BSAT is turned on to lubricate the Pelton wheel bearings.

Free-Spinning Compressed Air Driven Tests

To perform the free-spinning test, the air supply to the Barbour Stockwell air turbine was turned off to allow it to spin freely with the TurbX™ shaft. The gate valve feeding air to the spark plug port of the TurbX™ is now opened to initiate rotation. Once the TurbX™ has reached a steady speed at an input pressure of 138 kPa (20 psig), data were recorded. The data for this case represents a situation where the TurbX™ engine,

driven by compressed air, overcomes the parasitic load associated with the aerodynamic drag of the two pelton wheels of the BSAT, its rotational mass, and the frictional load of the BSAT and the Magtrol torque meter bearings. Additional data were acquired for input pressures of 207, 278 and 345 kPa to the spark plug port, thereby varying output speed.

Loaded Compressed Air Driven Tests

To perform the loaded test of TurbX™, the gate valve to supply air to the retarding Pelton wheel (i.e., secondary port) of the BSAT was opened. This enabled the BSAT to resist the motion of the TurbX™ engine. If TurbX™ were not energized, the BSAT would normally reverse its direction of rotation. However, with the air-driven TurbX™ driving the BSAT, the system rotates in the same direction as during the no-load condition. Basically, the BSAT is providing rotational resistance to TurbX™.

Data were recorded at the initial gauge pressure of 345 kPa, and continued at lower pressures until the TurbX™ stalled. This value was typically around 310 kPa gauge. For air pressures less than about 310 kPa, the TurbX™ could not sustain the load and no meaningful data could be obtained.

The above free-spinning and loaded test procedures were followed for gap settings of G_3, G_2, and G_1 (smallest). To demonstrate repeatability for the parasitic load data, tests were conducted on two consecutive days, totaling twenty separate test runs.

CHAPTER VI

RESULTS AND DISCUSSION

Air-driven tests were conducted on August 20th and 21st, 2001. After the 21st, the project had sufficient data to proceed to the next phase of the project, the fired test. The test setup had to be reconfigured before the fuel-fired tests could be conducted. A total of 20 tests was conducted to measure TurbX™ air driven characteristics as a function of inlet air pressure. The BSAT was used to initiate rotation of the engine during all air-driven tests. Airflow rate supplied to the BSAT was constant for each individual test, allowing the TurbX™ to spin at a constant speed.

The measured torque values fluctuated noticably and therefore data were recorded at 1 Hz for a period of 10 seconds. The results presented here are mean values over 10 readings recorded at each speed. The standard deviation of the 10 readings is used as the uncertainty of the torque measurement. The torque results presented represent standard deviations of 25 to 50% of the mean value. Therefore, the trends discussed are within the uncertainty limits of the data. It should be pointed out that in all the figures presented in this chapter, each straight line shown represents a linear least squares curve fit of the data associated with a particular gap setting.

Free-Spinning Test Results

As seen in Figure 6.1, when the TurbX™ engine is driven by compressed air, the rotational speed of the engine linearly increases with supply pressure to the combustion chamber. Clearly at the smallest gap G_1, the speeds are lower for almost all pressures compared to the higher gaps of G_2 and G_3. However, at higher pressures all gap settings result in approximately the same speed. This drop in speed for the smallest gap could be due to increased friction caused by non-planar alignment of one stator relative to the other stator. At this closest gap setting, the surface irregularities of the stator

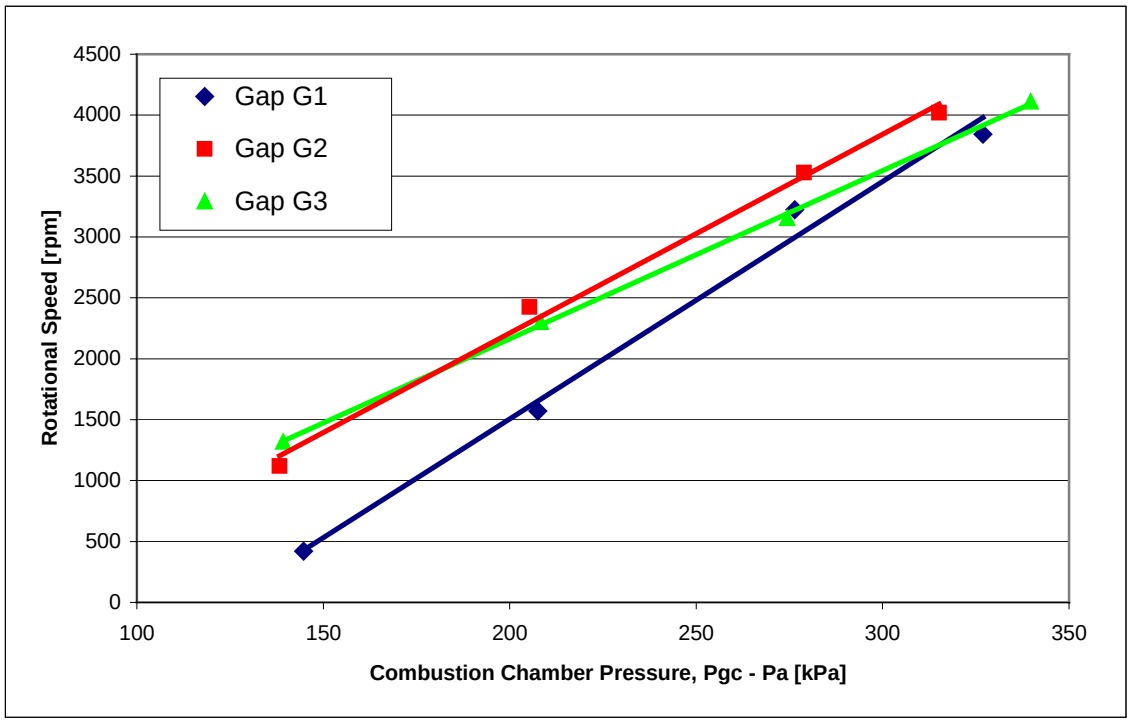

Figure 6.1. Free-Spinning Speed Characteristics of the Air-Driven TurbX™ Engine and the Testing System

surfaces facing the rotor could significantly increase frictional resistance, adding additional drag to the rotor.

In Figure 6.2 the temperature drop of the air as it expanded through the engine is shown as a function of the inlet air gauge pressure ($P_{gc} - P_a$). A maximum temperature drop of 10.4^{o}C from the inlet to the outlet of the engine was observed for the test conducted with a gap setting of G_1. This temperature drop is expected as air expands through the engine[6]. This change in temperature increased linearly as the pressure into the engine was increased for all gap settings. At the smallest gap, the temperature drops are lower for almost all pressures compared to the wider gaps of G_2 and G_3, particularly at low inlet pressures between 150 and 220 kPa. The reduced temperature drop for the

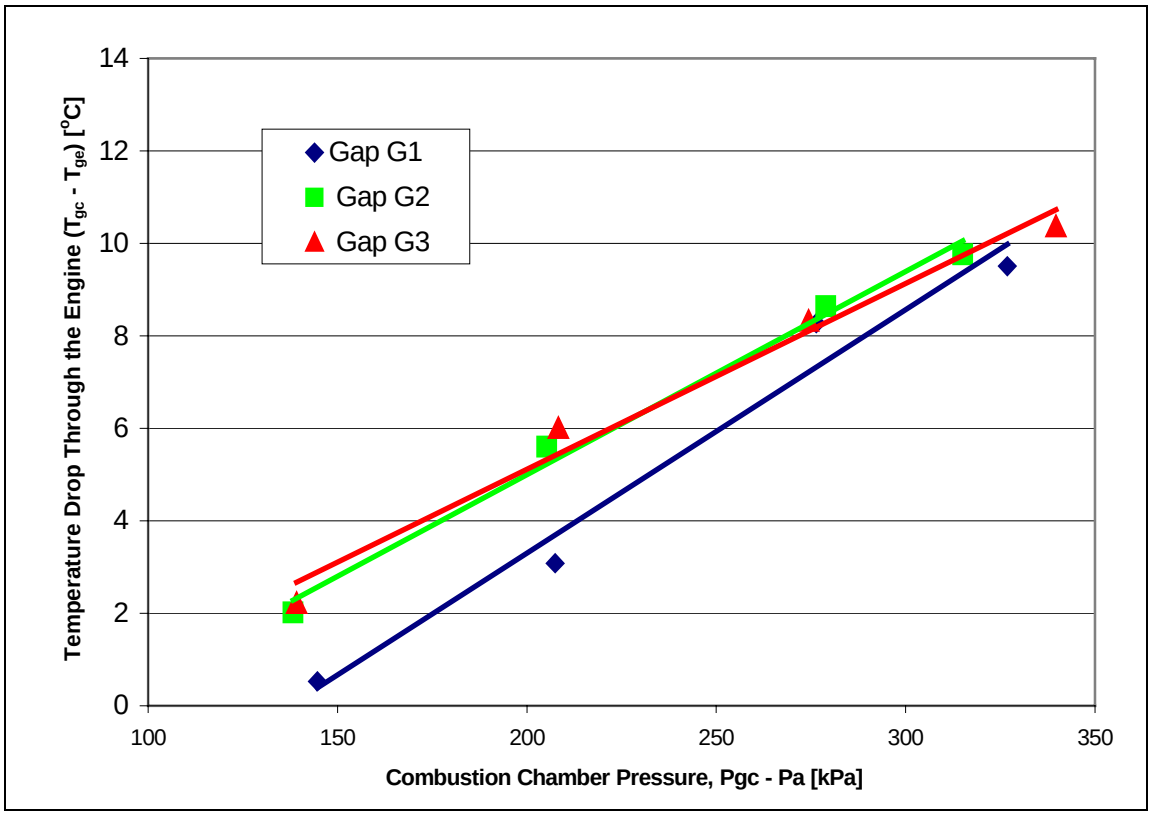

Figure 6.2. Free-Spinning Temperature Drop Characteristics of the Air-Driven TurbX™ Engine and the Testing System

smallest gap G_1 may be attributable to the increased effect of surface irregularities on the frictional resistance between the rotor and the stators. In other words, at this closest gap setting, the surface irregularities of the stator surfaces facing the rotor could significantly increase frictional resistance, resulting in frictional heating that reduced the air temperature drop.

In Figure 6.3, volumetric air flow rate is plotted as functions of inlet gauge pressure. The volumetric air flow rates plotted represent the *sum* of leakage air flow and air flow through the engine. When the gap is reduced from G_3 to G_2, flowrate is increased by 10% across the board. As the gap is tightened further from G_2 to G_1, the flow rate is *decreased* by 5%. This decrease could again be attributable to frictional resistance, causing the rotor to spin slower.

The torque measurements of the free-spinning air-driven TurbX™ engine and the testing system are shown in Figure 6.4. This torque is a characteristic that is likely to be more representative of the free-spinning BSAT and the associated parasitic load and it can be expected to be somewhat dependent upon speed. Additionally, the torque measurements were unsteady, and the uncertainties associated with the averaged torque values in Figure 6.4 were between 25% and 50%, as indicated earlier in this chapter. As a consequence, the trends shown in Figure 6.4 are all within the uncertainty bands and therefore no conclusions can be drawn with respect to gap on developed torque of the system.

Loaded Test Results

A typical *loaded* gas turbine expander would have a negative slope on the torque – speed plot [11]. This means that the turbine develops its maximum torque at lower speeds. While TurbX™ is not a typical gas turbine engine, the results shown in

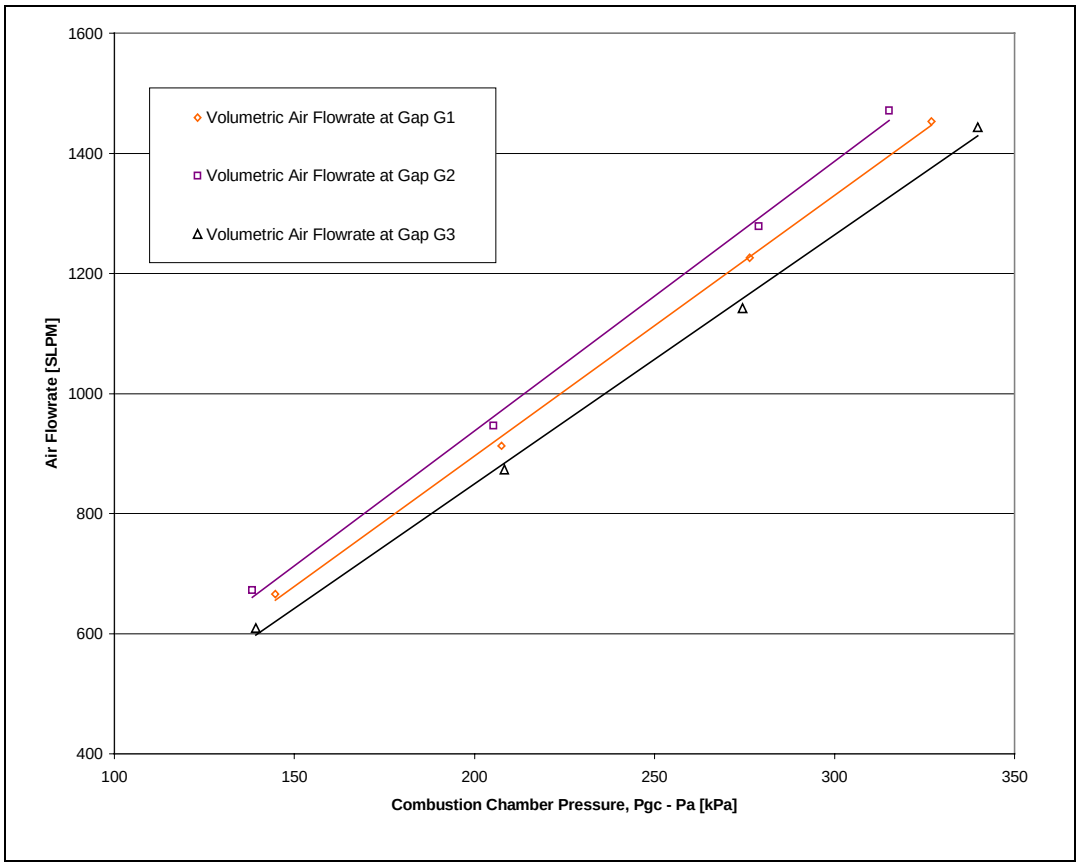

Figure 6.3. Free-Spinning Volumetric Air Flowrate Characteristics of the Air-Driven TurbX™ Engine and the Testing System

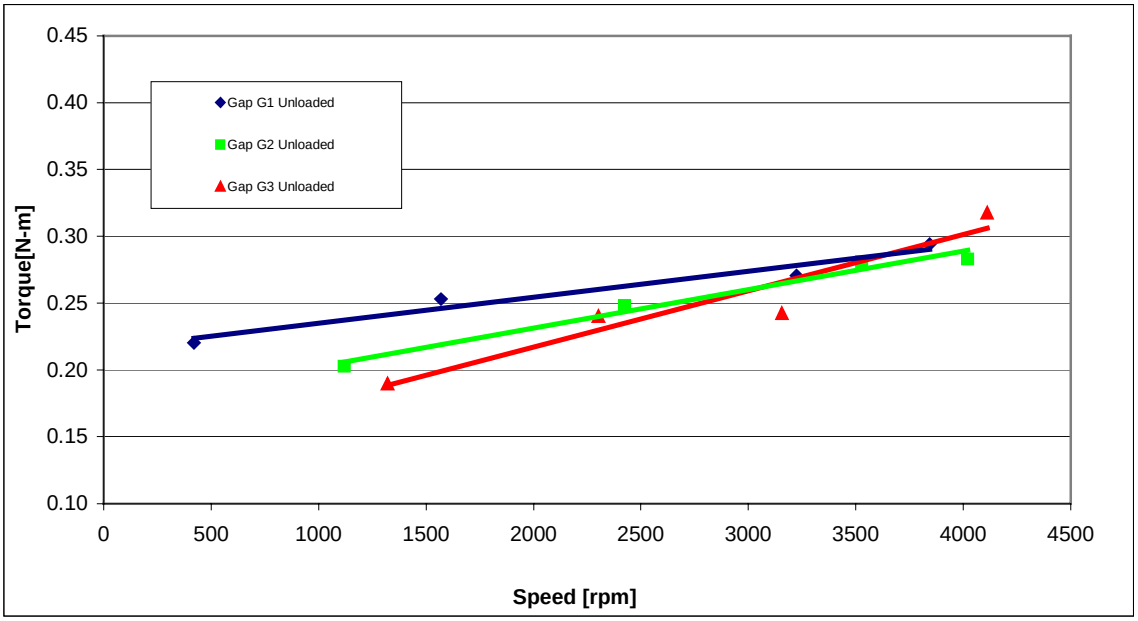

Figure 6.4. Free-Spinning Torque Characteristics of the Air-Driven TurbX™ Engine and the Testing System

Figure 6.5 indicate a similar trend. At gap G_1, as speed changes from 2,100 to 3,400 rpm, torque drops from 0.41 to 0.35 N-m. Similar trends, but at progressively lower levels of torque, can be seen for the other wider gap settings, G_2 and G_3. Increasing the gap width will decrease the torque levels at any given speed, primarily as a consequence of increased leakage flow. For even the tightest gap, G_1, the prototype TurbX™ did not produce a remarkable amount of torque. Maximum torque values observed were 0.41 N-m. More importantly however, as the gap is significantly narrowed, the TurbX™ performance may approach the performance of traditional gas turbine engines.

The presented trends indicate that, if leakage could be reduced, torque levels should increase. Leakage reduction is a very critical issue for cold flow performance, and this would be further complicated in fired test results by the presence of temperature gradients around the rotor and the stators. Also, inefficiencies in the blade angles were evident in cold flow testing, as observed by the audible siren-like high-pitched noise produced by the engine. Blade angle design should be improved to reduce the losses associated with poor air-incidence angles.

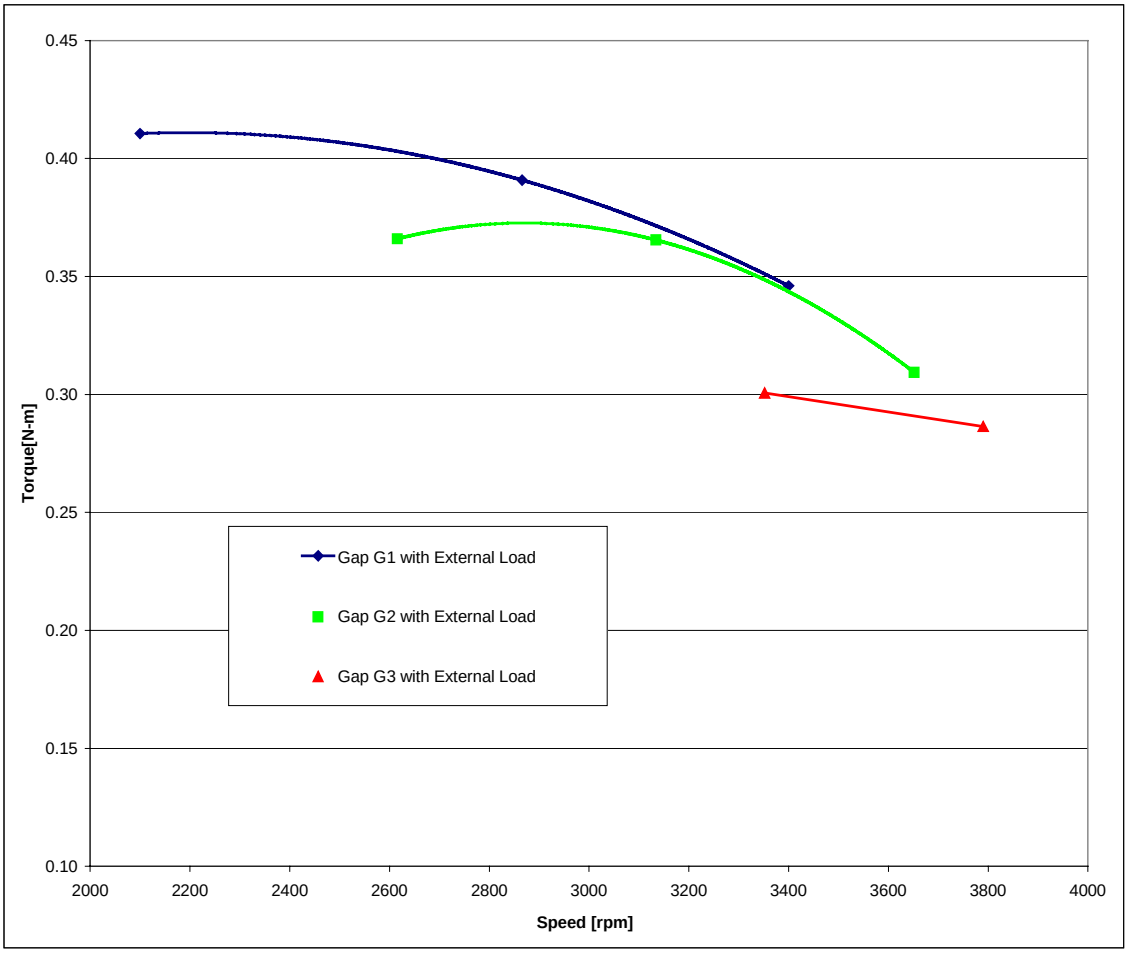

Figure 6.5. Loaded Torque Speed Plot for the TurbX™ Prototype

In summary, although air driven tests were limited to combustion chamber pressures of up to 345 kPa by the air supply system, the TurbX™ engine did not produce a remarkable amount of torque.

It would be of interest to know the value of T* on Figure 3.2 that corresponds to this maximum gauge pressure of 345 kPa. The value of T* can be related to maximum pressure by using the insentropic compression and constant volume heat addition process equations for ideal gases:

$$T^* = \frac{P_3}{P_1}\left(r_c\right)^{-\frac{1}{k}}$$

With the combustion chamber pressure, P_3 = 345 +101 kPa, P_1 = 101 kPa and a compression ratio of r_c = 1, this equation yields a T* value of 4.4. This value represents a single point on Figure 3.2, corresponding to a thermal efficiency of about 24%.

All the results reported here are recorded consistently over a 2-day interval without altering the test configuration. The frame mountings were not changed during the two-day test interval, and the instrumentation transducers and data acquisition system were not changed during the test interval.

CHAPTER VII

CONCLUSIONS

The goals of the study of the 15 kW prototype TurbX™ engine were to familiarize the project team with the prototype prior to fired testing, to determine appropriate test equipment within the resources available, and to conduct the air-driven tests. These goals were accomplished. The free-spinning tests indicated the speed increased linearly with pressure in the combustion chamber. The loaded tests showed that with a smaller gap setting, the engine had characteristics similar to those of gas turbine expanders, having a negative slope on the torque-speed plot.

The prototype was claimed by the inventor to produce 15 kW at a speed of 20,000 rpm. Although air-driven tests were limited to combustion chamber pressures of up to 345 kPa by the air supply system, the TurbX™ prototype did not produce a remarkable amount of torque. Low torque output in the loaded air driven tests is also indicative of the excessive leakage through the rotor/stator gap in the blading section of the rotor. Further development and research is needed to address this serious problem.

Based on the results of the air driven tests and the experience gained, several recommendations can be made. Some of them are simple lessons learned while testing, while others are complex design issues that must be addressed in order for this engine to be viable. Following are the recommendations in the order of increased complexity:

1. Future testing of the engine should be done with a horizontal axis of rotation. This orientation should eliminate the need for high air bearing pressure to lift the rotor off the bottom stator, as was the case in the present test. This orientation is also more indicative of typical applications of modern engines.
2. Future testing of new TurbX™ designs should use a different dynamometer to make testing easier. One recommendation would be an AC vector drive electric

motor dynamometer perhaps coupled with a speed-reducing gearbox. This type of dynamometer has touch screen controls and will measure torque and output shaft speed, all in one package. The BSAT demanded a high volume of air and was difficult to control with gate valves regulating pressure to the Pelton wheel. Moreover, when the shop-supplied air to the BSAT is from the same source as the inlet to TurbX™, the load developed by the BSAT fluctuated. This is yet another recommendation for this recommendation.

3. Future TurbX™ design changes should have better gap control between the rotor and two stators.

4. Inefficiencies in the blade angles were evident in cold flow testing due to low measureed torque.

5. The excessive noise, as observed by the audible siren-like high-pitched noise produced should be reduced.

6. Blade angle design should be improved to reduce the losses associated with poor air-incidence angles.

7. TurbX™ designers will eventually have to address issues related to the cooling system. This might increase the engine weight and bring the power-to-weight ratio of the engine closer to values representative of modern day power plants.

LIST OF REFERENCES

LIST OF REFERENCES

1. Wilson, Michael W., "Efficiency Enhanced Turbine Engine." US Patent Number 5,966,927, October 19, 1999.

2. Wilson, Michael W., "Efficiency Enhanced Turbine Engine." US Patent Number 6,105,359, August 22, 2000.

3. Theiss, T.J., Conklin, J.C., Thomas, J.F., Armstrong, T.R., "Comparison of Prime Movers Suitable for USMC Expeditionary Power Sources." ORNL/TM-2000/116, Oak Ridge National Laboratory March 2000.

4. Heywood, J.B., 1988, "Internal Combustion Engine Fundamentals." McGraw-Hill, New York, NY.

5. Erickson, Kurt, "Determination of the Performance of a Prototype TurbX™ Engine." Thesis. University of Tennessee. August 2002.

6. Moran, M.J. and Shapiro, H.N., 1995, "Fundamentals of Engineering Thermodynamics." 3rd Edition, John Wiley and Sons, NY.

7. Venturini, Osvaldo Jose, and Varella, Sebastiao, "A Reevaluation of the Holzwarth Gas Turbine Cycle for Use in Small Power Plants." ASME Paper 2001-GT-547, internal Gas Turbine and Aeroengine Congress & Exhibition, New Orleans, USA, June 2001.

8. Hutchins, T.E. and Metghalchi, M. "Energy and Exergy Analysis of the Pulse Detonation Engine." Journal of Engineering for Gas Turbines and Power. Volume 125. American Society of Mechanical Engineers. October 2003.

9. National Instruments Corporation, "Measurement and Automation Catalog." Austin, TX, 2001.

10. SolidWorks® 97, SolidWorks Corporation, Concord, MA, 1997.

11. Wilson, D.G., and Korakianitis, T., 1998, "The Design of High-Efficiency Turbomachinery and Gas Turbines." 2nd Edition, Prentice-Hall, NJ.

APPENDICIES

APPENDIX A

DEADLINES AND PROCUREMENT ISSUES

The deadline to complete the unfired and fired testing of the engine was September 30, 2001. At that point the testing bay at the NTRC had to be evacuated and cleared of all instrumentation and testing apparatus associated with the project. Safety procedures approved by ORNL were written and followed throughout all the testing sequences.

The NTRC in-house screw-type air compressor did not deliver the flow rate required for optimal speed testing of the engine as well as handle the demands of the BSAT turbine. Furthermore, no accumulator for the compressor was available, as usually seen in the industry. The only "accumulator" was the 0.5 inch steel air lines running throughout the building. The project was thus limited in the duration of each testing sequence. After roughly 5 minutes, the air pressure dropped significantly in the system, enough to trigger the safety switch for the screw-compressor. At one point the project even considered renting a portable engine-driven compressor, often found at construction job sites, to make up for the loss.

APPENDIX B

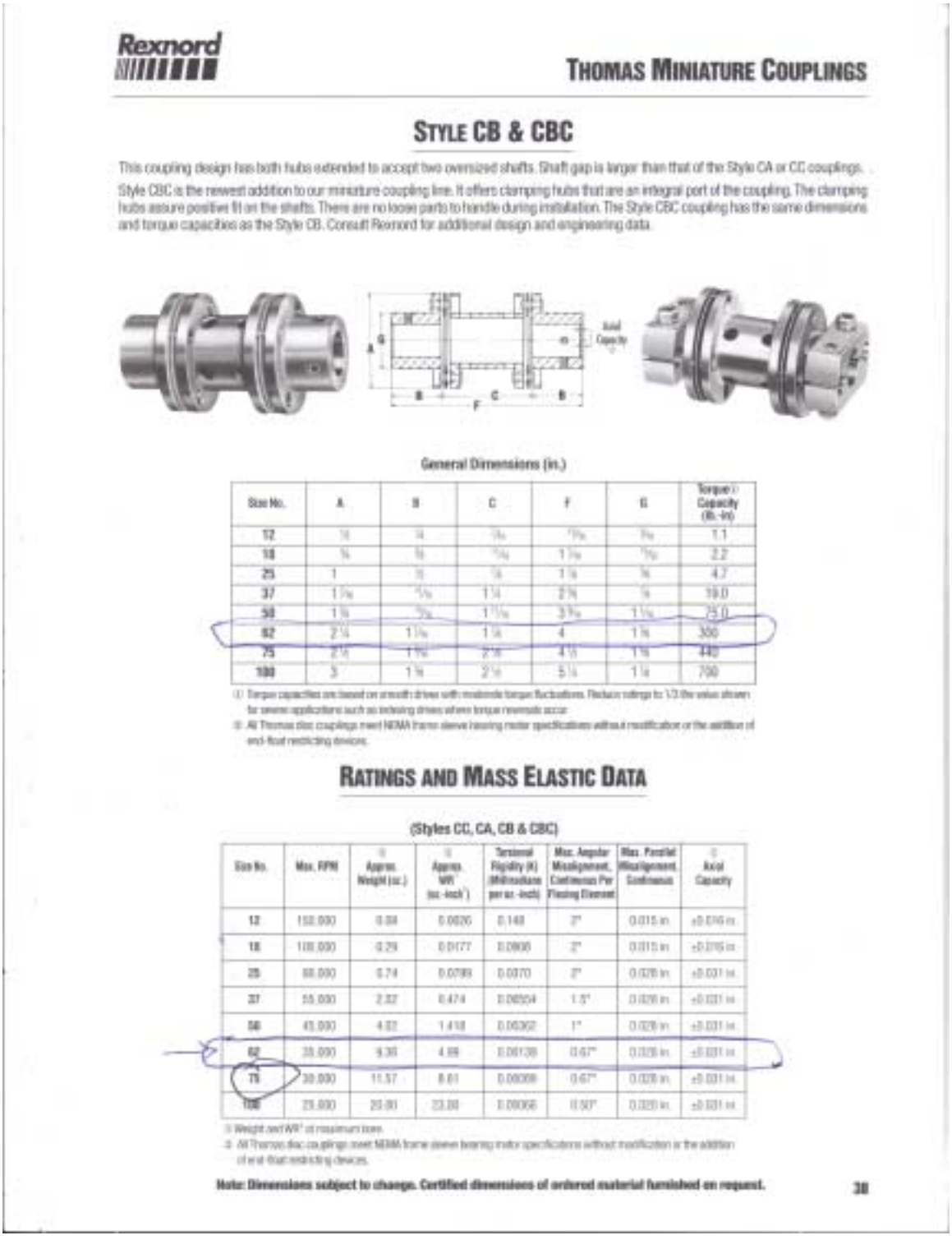

Rexnord

THOMAS MINIATURE COUPLINGS

STYLE CB & CBC

This coupling design has both hubs extended to accept two oversized shafts. Shaft gap is larger than that of the Style CA or CC couplings.

Style CBC is the newest addition to our miniature coupling line. It offers clamping hubs that are an integral part of the coupling. The clamping hubs assure positive fit on the shafts. There are no loose parts to handle during installation. The Style CBC coupling has the same dimensions and torque capacities as the Style CB. Consult Rexnord for additional design and engineering data.

General Dimensions (in.)

Size No.	A	B	C	F	G	Torque ① Capacity (lb.-in)
12	½	¼	⅜	1⅜	⅜	1.1
18	¾	⅜	¼	1⅝	⅝	2.2
25	1	½	⅝	1⅞	¾	4.7
37	1⅜	⅝	1¼	2⅜	¾	19.0
50	1½	⅞	1⅜	3⅛	1⅛	25.0
62	2¼	1⅛	1⅞	4	1⅜	300
75	2½	1⅜	2⅛	4½	1⅜	440
100	3	1⅜	2½	5¼	1⅜	700

① Torque capacities are based on smooth drives with moderate torque fluctuations. Reduce ratings to 1/3 the value shown for severe applications such as reversing drives where torque reversals occur.

② All Thomas disc couplings meet NEMA frame sleeve bearing motor specifications without modification or the addition of end-float restricting devices.

RATINGS AND MASS ELASTIC DATA

(Styles CC, CA, CB & CBC)

Size No.	Max. RPM	① Approx. Weight (oz.)	① Approx. WR² (oz.-inch²)	Torsional Rigidity (K) (Millionsdane per oz.-inch)	Max. Angular Misalignment, Continuous Per Flexing Element	Max. Parallel Misalignment, Continuous	① Axial Capacity
12	150,000	0.09	0.0020	0.148	2°	0.015 in.	±0.016 in.
18	100,000	0.29	0.0177	0.0900	2°	0.015 in.	±0.016 in.
25	80,000	0.74	0.0789	0.0370	2°	0.020 in.	±0.031 in.
37	55,000	2.02	0.474	0.00504	1.5°	0.020 in.	±0.031 in.
50	45,000	4.02	1.418	0.00302	1°	0.020 in.	±0.031 in.
62	35,000	9.36	4.88	0.00139	0.67°	0.020 in.	±0.031 in.
75	30,000	11.57	8.61	0.00099	0.67°	0.020 in.	±0.031 in.
100	25,000	20.00	23.00	0.00056	0.50°	0.020 in.	±0.031 in.

① Weight and WR² at maximum bore.

② All Thomas disc couplings meet NEMA frame sleeve bearing motor specifications without modification or the addition of end-float restricting devices.

Note: Dimensions subject to change. Certified dimensions of ordered material furnished on request.

38

Figure B.1. Thomas Miniature Couplings Data Sheet

APPENDIX C

INITIAL CALCULATIONS FOR ESTIMATION OF AIRFLOW RATE THROUGH TURBX

Calculation for the mass flow rate and volumetric flow rate of fuel and air are calculated for the TurbX™ engine below.

Assumptions:

$P_{out} \approx 20\,hp = 14.9\,kW$, Theoretical shaft power out given by the inventor

$\eta_{th} \approx 35\%$

$HHV_{CH_4} = 55\ \frac{MJ}{kg}$, Higher heating value of gaseous methane

$LHV_{CH_4} = 50\ \frac{MJ}{kg}$, Lower heating value of gaseous methane

$$\eta_{th} = \frac{P_{out}}{\dot{m}_f (HV)}$$

For determining the range required of the laminar flow meter, the mass airflow rate is estimated using stochiometric combustion:

Stochiometric Air/Fuel ratio for CH_4 = 17.23

Molecular weight of CH_4 = 16.04

$$\dot{m}_f = \frac{P_{out}}{\eta_{th} \cdot (HV)}$$

Then:

$$\dot{m}_f = \frac{14.9\ kW\ kg}{0.35 \cdot 50\ MJ} \times \frac{1\ MJ}{1000\ kJ} \times \frac{1\ kJ}{1\ kW \cdot s} = 8.514 \times 10^{-4}\ \frac{kg}{s}$$

$$\dot{m}_f = 8.514 \times 10^{-4}\ \frac{kg}{s} \times \frac{60\ s}{1\ \text{min}} = 0.0510\ \frac{kg}{\text{min}} = 51.0\ \frac{g}{\text{min}}$$

What is the volumetric flow rate of the fuel?

$$\dot{m}_f = \rho A V$$

$$AV = \frac{\dot{m}_f}{\rho}$$

Assume:
$T = 298\ K$
$p = 1\ atm$

$$\rho = \frac{p}{RT}$$

Then:

$$\rho_{CH_4} = \frac{100\ kPa}{\left(8.314 \frac{kJ}{kmol \cdot K}\right) \cdot 298\ K \left(\frac{1 kmol}{16.04 kg}\right)} = 0.647 \frac{kg}{m^3}$$

Calculate the volumetric flow rate of the fuel, $\dot{V}_f$:

$$\dot{V}_f = \frac{\dot{m}_f}{\rho}$$

$$\dot{V}_f = \frac{0.0510 \frac{kg}{\min}}{0.647 \frac{kg}{m^3}} = 0.0788 \frac{m^3}{\min} = 2.78 \frac{ft^3}{\min} = 78.8 \frac{L}{\min}$$

What is the volumetric flow rate of air, $\dot{V}_a$?

$$\dot{V}_a = \left.\frac{A}{F}\right|_{stoch} \times \dot{V}_f$$

$$\dot{V}_a = 17.23 \times\ 0.788 \frac{m^3}{\min} = 1.357 \frac{m^3}{\min} = 1357 \frac{L}{\min}$$

$$\boxed{\dot{V}_a = 1357 \frac{L}{\min}}$$

APPENDIX D

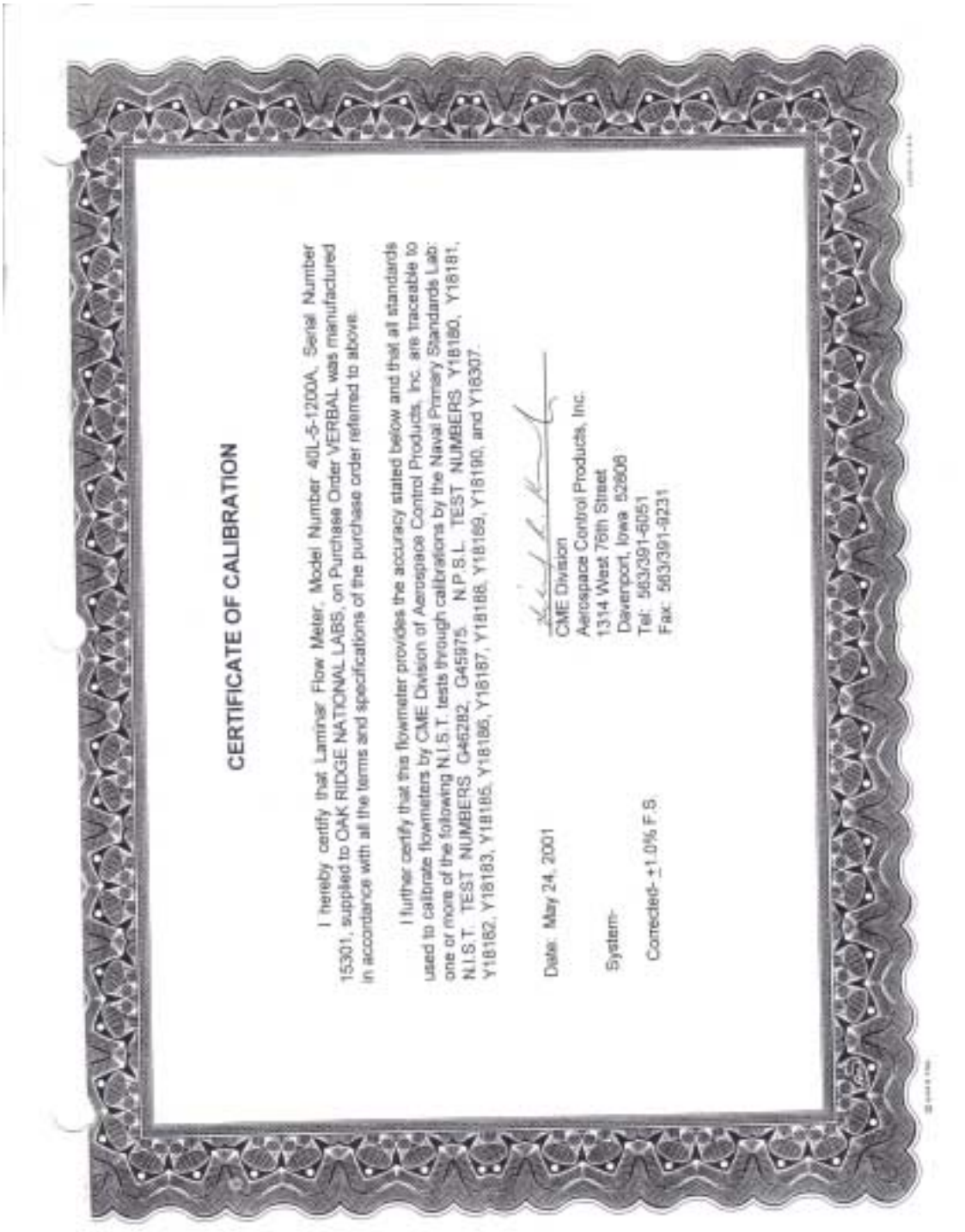

CERTIFICATE OF CALIBRATION

I hereby certify that Laminar Flow Meter, Model Number 40L-5-1200A, Serial Number 15301, supplied to OAK RIDGE NATIONAL LABS, on Purchase Order VERBAL was manufactured in accordance with all the terms and specifications of the purchase order referred to above.

I further certify that this flowmeter provides the accuracy stated below and that all standards used to calibrate flowmeters by CME Division of Aerospace Control Products, Inc. are traceable to one or more of the following N.I.S.T. tests through calibrations by the Naval Primary Standards Lab: N.I.S.T. TEST NUMBERS G46282, G45975 N.P.S.L. TEST NUMBERS Y18180, Y18181, Y18182, Y18183, Y18185, Y18186, Y18187, Y18188, Y18189, Y18190, and Y18307.

Date: May 24, 2001

System-

Corrected- +1.0% F.S.

CME Division
Aerospace Control Products, Inc.
1314 West 76th Street
Davenport, Iowa 52806
Tel: 563/391-6051
Fax: 563/391-9231

Figure D.1. Laminar Flow Meter Calibration Certificate

APPENDIX D

CALIBRATION DATA

USTOMER: OAK RIDGE NAT'L LABORATORIES

ODEL #: 40L-S-1200A

AS: AIR

EST: FINAL

DATE: 5/24/01

S/N: 15301

F.S. FLOW: 1200 LPM

CALIBRATION DUE: 5/24/02

AROMETRIC PRESSURE: 28.963" HgA

CME LAB STD. LS1000 **S/N 15301**

TEMP. (DEG. F.)	LAB STD. (SLPM)	M40L (SLPM)	DEV. (SLPM)	PCT. F.S.
70.2	1167.0	1165.0	2.0	0.17%
70.6	589.0	588.0	1.0	0.08%
70.5	117.8	117.0	0.8	0.07%

CME DIVISION, AEROSPACE CONTROL PRODUCTS, INC.
1314 W. 76TH STREET, DAVENPORT, IOWA (319) 391-6051 FAX (319) 391-9231

Figure D.2. Laminar Flow Meter Calibration Information

APPENDIX E

SAFETY CONCERNS OF THE UNFIRED TESTS

This test was conducted at the NTRC and the center's safety compliance requirements had to be satisfied before tests could be initiated. NTRC staff conducted several independent reviews during the design and fabrication phases of the project. Some of the safety concerns addressed for the unfired tests are related to rotational dangers, audible hazards, and the use of compressed air as a primary driving fluid. These are discussed below.

Rotational Dangers:

Rotor stresses of TurbX™ were estimated to check the practicality of operating at 18,000 rpm. A rotor radius of 70 mm and a rotor tip speed of 132 m/s was assumed to get 18,000 rpm. A 17 mm shaft hole was also assumed. For a simple flat disk with a center hole but without blades, the maximum rotational stress is estimated to be below the annealed yield strength for Invar-36 of 70 ksi. The Invar rotor should hold together at least for short duration demonstration tests. As there was no cooling of the stators, the short duration runs should not result in temperatures high enough to approach the 2600 ^{o}F melting temperature of Invar.

Audible Hazards:

When the TurbX engine is air–driven at 5,000 rpm without any ductwork on the exhaust stream, the engine sounded much like a small siren. To meet the safe noise standards, NTRC safety compliance staff mandated that hearing protection be worn by all during the test.

The BSAT is also a source of noise pollution. To overcome this hazard, a muffler is placed in series after the oil separator to reduce the overall impact of audible noise to personnel. With the combined siren effects of TurbX™ and the BSAT, double ear insulation has been recommended.

Compressed Air:

Compressed air will have two vital roles for the success of the project. Both of these roles need to be handled with care. Potential safety concerns were related to compressed air usage and the expected high-speed (20,000 rpm) operation of the system. Safety procedures of the NTRC had to be observed. In the unfired test, air will be the "fluid" driven through the engine. The inlet air duct of the engine will be blocked off, and all air will be forced through the spark ignition port. This air will be supplied by the NTRC screw type air compressor, capable of delivering up to 220 cfm at 100 psig.

The other role compressed air plays was to supply pressure to the BSAT turbine wheel. Two lines of compressed air were placed, feeding the turbine. The turbine is actually made up of two coaxial, counter-rotating, impulse turbine wheels. One air supply line is routed to the primary driver, used to spin the dynamometer in the clockwise direction (from above), the only direction the TurbX™ engine should spin. The other air supply line will be the secondary driver, providing pressure to the turbine wheel with buckets facing the opposite direction, thus braking and controlling the speed of the turbine.

APPENDIX F

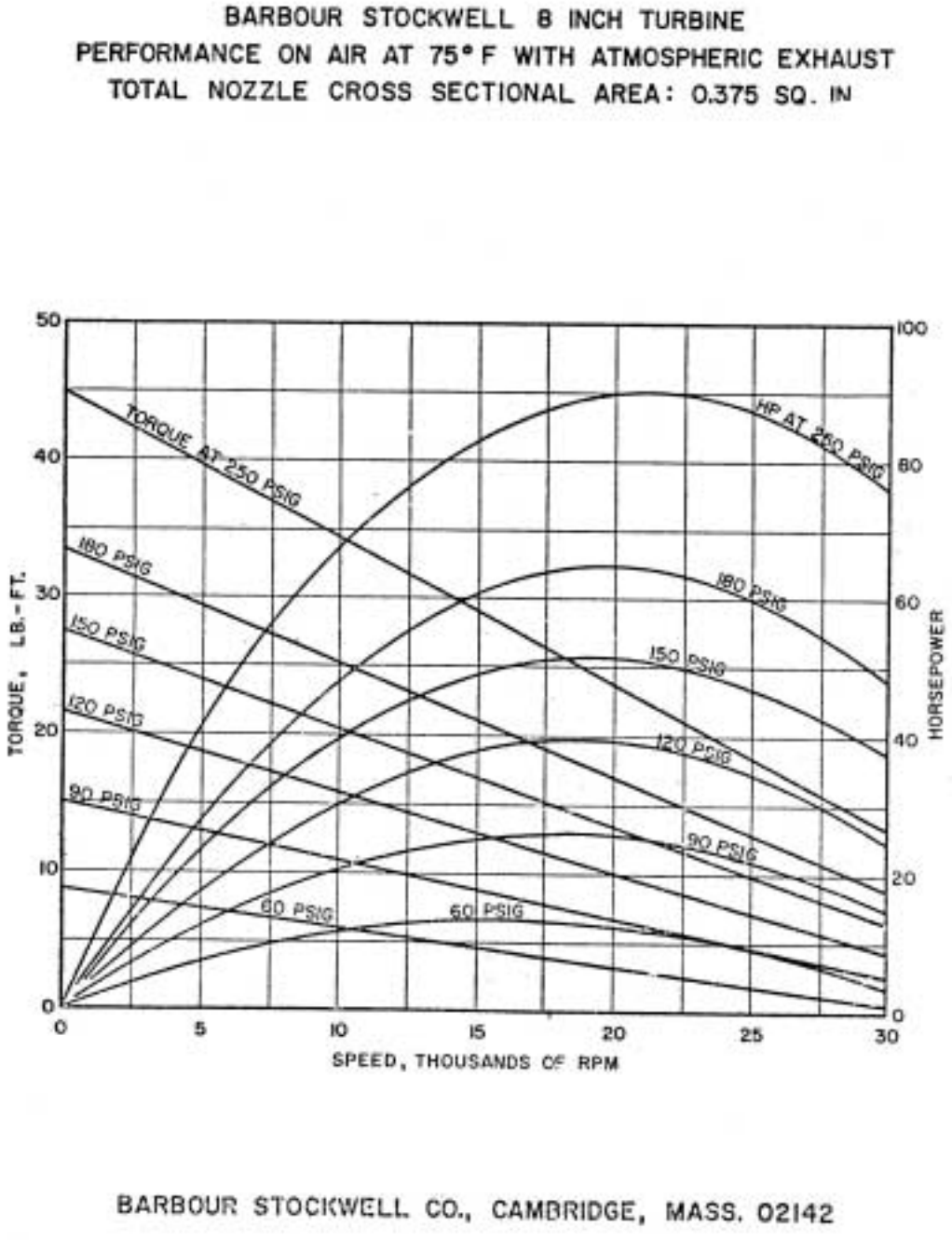

Figure F.1. Barbour Stockwell Air Turbine Dynamometer Performance

VITA

Frederick John Mottley was born in Nashville, TN on November 30, 1975. Fred attended the Farragut High School system, in Farragut, TN where he graduated in the spring of 1994. He enrolled in the University of Tennessee, Knoxville the following fall to study mechanical engineering. For his first three years, Fred worked alternating semesters as a Co-op student throughout his undergraduate studies as a System Engineer at the Grand Gulf Nuclear Power Plant, in Port Gibson, MS. In his junior year, he accepted a position to assist researchers from Oak Ridge National Labs (ORNL), who were conducting research in the area of diesel engine emissions. In 1999, Fred pursued an interest in research and design of hybrid electric vehicles with UT's FutureCar Team as the engine group's leader. Fred was also the Society of Automotive Engineers (SAE) student chairperson of the UT chapter in 1999, and was also awarded the Mechanical Engineering Department Head's "Outstanding Senior Award" his last year.

As seen from his developing leadership skills and scholastic performance, Fred was awarded a fellowship at the University of Tennessee in the fall of 1999 through the Graduate Automotive Technology Education (GATE) program to pursue a Master of Science degree in Mechanical Engineering. The GATE program was funded by DOE, and focused on accelerating advancements in Hybrid Electric Vehicle theory and design.

Through his contacts with ORNL and the GATE program, Fred was asked to perform the analysis on the TurbX engine jointly with UT and ORNL engineers.

Fred currently works with the US DOT at the Volpe Transportation Systems Research Center in Cambridge, MA and is happily married to his wife Kimberly, where they currently live in Boston with their dog, Mickey.